

Hadron production in heavy ion collisions: Fragmentation and recombination from a dense parton phase

R. J. Fries, B. Müller, and C. Nonaka

Department of Physics, Duke University, Durham, North Carolina 27708, USA

S. A. Bass

Department of Physics, Duke University, Durham, North Carolina 27708, USA and RIKEN BNL Research Center, Brookhaven National Laboratory, Upton, New York 11973, USA

(Received 12 June 2003; published 24 October 2003)

We discuss hadron production in heavy ion collisions at the Relativistic Heavy Ion Collider (RHIC). We argue that hadrons at transverse momenta $P_T < 5$ GeV are formed by recombination of partons from the dense parton phase created in central collisions at RHIC. We provide a theoretical description of the recombination process for $P_T > 2$ GeV. Below $P_T = 2$ GeV our results smoothly match a purely statistical description. At high transverse momentum hadron production is well described in the language of perturbative QCD by the fragmentation of partons. We give numerical results for a variety of hadron spectra, ratios, and nuclear suppression factors. We also discuss the anisotropic flow v_2 and give results based on a flow in the parton phase. Our results are consistent with the existence of a parton phase at RHIC hadronizing at a temperature of 175 MeV and a radial flow velocity of $0.55c$.

DOI: 10.1103/PhysRevC.68.044902

PACS number(s): 25.75.Dw, 24.85.+p

I. INTRODUCTION

Recent data from the Relativistic Heavy Ion Collider (RHIC) have shown a strong nuclear suppression of the pion yield at transverse momenta larger than 2 GeV/ c in central Au + Au collisions, compared to $p+p$ interactions [1]. This is widely seen as the experimental confirmation of jet quenching, the phenomenon that high energy partons lose energy when they travel through the hot medium created in a heavy ion collision [2–4], entailing a suppression of intermediate and high P_T hadrons.

However, the experiments at RHIC have provided new puzzles. The amount of suppression seems to depend on the hadron species. In fact, in the production of protons and antiprotons between 2 and 4 GeV/ c the suppression seems to be completely absent. Generally, pions and kaons appear to suffer from a strong energy loss while baryons and antibaryons do not. Two stunning experimental facts exemplify this [5–8]. First, the ratio of protons over positively charged pions is equal to or above 1 for $P_T > 1.5$ GeV/ c and is approximately constant up to 4 GeV/ c . Second, the nuclear suppression factor R_{AA} below 4 GeV/ c is close to 1 for protons and lambdas, while it is about 0.3 for pions.

There have been recent attempts to describe the different behaviors of baryons and mesons through the existence of gluon junctions [9] or alternatively through recombination as the dominant mechanism of hadronization [10,11]. The recombination picture has attracted additional attention due to the observation that the elliptic flow pattern of different hadron species can be explained by a simple recombination mechanism [12–15]. The anisotropies v_2 for the different hadrons are compatible with a universal value of v_2 in the parton phase, related to the hadronic flow by factors of 2 and 3 depending on the number of valence quarks [16].

In this work we elaborate on the arguments presented in Ref. [10]. We will present the formalism as well as new

numerical results. The competition between recombination and fragmentation delays the onset of the perturbative/fragmentation regime to relatively high transverse momentum of 4–6 GeV/ c , depending on the hadron species. This is the explanation for several key observations at RHIC.

(i) The two component form of hadron transverse momentum spectra, including an exponential part and a power law tail with a transition between 4 and 6 GeV/ c .

(ii) The very different behavior of the nuclear suppression factors R_{AA} of mesons and baryons.

(iii) The particle dependence of the elliptic flow.

(iv) The unusually large baryon/meson ratios.

In addition, our calculation clarifies the range of applicability of perturbative calculations including energy loss.

The paper is organized as follows. In the following section we explain why fragmentation might not be the dominant mechanism of hadronization at intermediate transverse momenta of a few GeV/ c in heavy ion collisions. We discuss the fundamental principles of recombination and fragmentation. In Sec. III we present the theoretical framework of recombination in more detail and also discuss its shortcomings. In particular, we address the question of applicability at low transverse momentum. In Sec. IV we introduce our parametrization of the parton spectrum and discuss further calculational details, and in Sec. V we present numerical results on spectra, hadron ratios, nuclear suppression, and elliptic flow. Section VI summarizes our work.

II. FRAGMENTATION VERSUS RECOMBINATION

A. Fragmentation of partons

Inclusive hadron production at sufficiently large momentum transfer can be described by perturbative quantum chro-

modynamics (pQCD). The invariant cross section for a hadron h with momentum P can be given in factorized form [17],

$$E \frac{d\sigma_h}{d^3P} = \sum_a \int_0^1 \frac{dz}{z^2} D_{a \rightarrow h}(z) E_a \frac{d\sigma_a}{d^3P_a}. \quad (1)$$

The sum runs over all parton species a and σ_a is the cross section for the production of parton a with momentum $P_a = P/z$. Thus the parton production cross section has to be convoluted with the probability that parton a fragments into hadron h . The probabilities $D_{a \rightarrow h}(z)$ are called fragmentation functions [18]. Like parton distributions they are nonperturbative quantities. However, they are universal and once measured, e.g., in e^+e^- annihilations, they can be used to describe hadron production in other hard QCD processes.

Using Eq. (1) we can estimate the ratio of protons and pions. Taking, e.g., the common parametrization of Kniehl, Kramer, and Pötter (KKP) [19], the ratio $D_{a \rightarrow p}/D_{a \rightarrow \pi^0}$ is always smaller than 0.2 for each parton a . This reflects the well known experimental fact that pions are much more abundant than protons in the domain where pQCD is applicable. The excess of pions over protons even holds down to very low P_T , smaller than 1 GeV, where perturbative calculations are no longer reliable. In that domain one can argue that the difference in mass, $M_p \gg M_\pi$, lays a huge penalty on proton production. The small value of the p/π^0 ratio predicted by these calculations over the entire range of P_T is the reason why the ratio $p/\pi^0 \sim 1$ measured at RHIC is so surprising.

It has been suggested that the fragmentation functions $D_{a \rightarrow h}(z)$ can be altered by the environment [20,21]. The energy loss of the propagating parton in the surrounding medium leads, in first approximation, to a rescaling of the variable z . This would affect all produced hadrons in the same way, and thus cannot explain the observations at RHIC. In a picture with perturbative hadron production and jet quenching alone, the different behavior of hadrons cannot be described by one consistent set of energy loss parameters. To save the validity of the purely perturbative approach, species dependent nonperturbative contributions to the fragmentation functions have to be introduced *ad hoc* to explain the data [22].

Perturbative hadron production consists of three steps: production of a parton in a hard scattering, propagation and interaction with a medium, and finally hadronization of the parton. Only modifications in our understanding of hadronization are able to provide an explanation of the experimental observations, since the other steps are blind to the hadron species that will eventually be created.

B. From fragmentation to recombination

For the production of a hadron with momentum P via fragmentation we need to start with a parton with momentum $P/z > P$. The fragmentation functions favor very small values of z , i.e., the situation where the energy of the fragmenting parton is not concentrated in one hadron. On the other hand, the transverse momentum spectrum of partons is steeply fall-

ing with P_T . This makes it clear that fragmentation is a rather inefficient mechanism for the production of high P_T hadrons, since it has to overcome the limited availability of partons at even higher transverse momentum. As a result, the average $\langle z \rangle$ is larger than what is expected from the shape of the fragmentation functions. For pion production, $\langle z \rangle$ is about 0.6 for the production from a valence quark, 0.4 for a sea quark, and 0.5 for a gluon in the range $2 \text{ GeV}/c \leq P_T \leq 10 \text{ GeV}/c$ for leading order KKP fragmentation functions.

An outgoing high energy parton is not a color singlet and will therefore have a color string attached. The breaking of the string will initiate the creation of quark-antiquark pairs until there is an entire jet of partons, which have to share the energy of the initial parton. They will finally turn into many hadrons. If phase space is already filled with partons, a single parton description might not be valid anymore. Instead one would have to introduce higher twist (multiple parton) fragmentation functions. In the most extreme case, if partons are abundant in phase space, they might simply recombine into hadrons. This means that a u and a \bar{d} quark that are “close” to each other in phase space can bind together to form a π^+ . The scale of being close will be set by the width of the pion wave function. In this scenario the total pion momentum will be just the sum of the individual quark momenta. We immediately notice that this recombination mechanism is very efficient for steeply falling spectra: in order to produce a 5 GeV pion we can start with two quarks having (on average) about 2.5 GeV/ c transverse momentum and each being therefore far more abundant (on average) than a 10 GeV/ c parton that could produce the pion via fragmentation. Of course the recombining partons must be close in phase space, i.e., recombination will be suppressed if the phase-space density is low.

Recombination can be interpreted as the most “exclusive” form of hadronization, the end point of a hypothetical resummation of fragmentation processes to arbitrary twist. We cannot achieve a quantitative understanding of this at the moment. However, we can try to find an effective description which can be tested against observable consequences. In this work we will advocate a simple model for recombination and compare it with single parton fragmentation. These two mechanisms of hadron production compete differently depending on the phase-space density of partons. From the above we understand that the competition between fragmentation and recombination is dominated by the slope and the absolute value of the phase-space distribution of partons. Below we show that recombination always wins over fragmentation for an exponentially falling parton spectrum, but that fragmentation takes over if the spectrum has the form of a power law, as it is provided by pQCD. We will apply this insight to hadron production in relativistic heavy ion collisions at midrapidity and transverse momenta of a few GeV/ c where we expect a densely populated phase space. For the recombination of three quarks into a proton the momenta of three partons have to be added up, but only two momenta in the case of a pion. Assuming an exponential parton spectrum this implies for a proton a distribution $\sim [\exp(-P_T/3)]^3$ and for pions $\sim [\exp(-P_T/2)]^2$, predicting a constant p/π^+ ratio where the value is determined by simple counting of quan-

tum numbers [10]. We will show that some of the surprising experimental results from RHIC can be explained in this way.

C. The recombination concept

The idea of quark recombination was proposed long ago to describe hadron production in the forward region of $p+p$ collisions [23]. This was later justified by the discovery of the leading particle effect, the phenomenon that, in the forward direction of a beam of hadrons colliding with a target, the production of hadrons sharing valence quarks with the beam hadrons is favored. For example, in the Fermilab E791 fixed target experiment with a 500 GeV π^- beam [24] the asymmetry

$$\alpha(x_F) = \frac{d\sigma_{D^-}/dx_F - d\sigma_{D^+}/dx_F}{d\sigma_{D^-}/dx_F + d\sigma_{D^+}/dx_F} \quad (2)$$

between D^- and D^+ mesons grows nearly to unity when the Feynman variable x_F , measuring the longitudinal momentum relative to the beam momentum, approaches 1. Fragmentation would predict this asymmetry to be very close to zero. However, recombination of the \bar{c} quark from a $c\bar{c}$ pair produced in a hard interaction with a d valence quark from the π^- , propagating in forward direction with large momentum, is highly favored compared to the recombination of the c with a \bar{d} which is only a sea quark of the π^- . This leads to the enhancement of D^- over D^+ mesons in the forward region.

The leading particle effect is a clear signature for the existence of recombination as a hadronization mechanism and has been addressed in several publications recently [25,26]. In this case recombination is favored over fragmentation only in a certain kinematic situation (the very forward direction), which is a only small fraction of phase space.

In central heavy ion collisions many more partons are produced than in collisions of single hadrons. The idea that recombination may then be important for a wide range of rapidities—and at least up to moderate transverse momenta—was advocated before [27–29]. However, it was only recently that RHIC data indicated that recombination could indeed be a valid approach up to surprisingly high transverse momenta of a few GeV/ c .

Charm and heavy hadron production have the advantage that the heavy quark mass provides a large scale that permits a more rigorous treatment of the recombination process [26]. The description of recombination into pions and protons seems to be theoretically less rigorous. However, a simple counting of quantum numbers in a picture where the structure of hadrons is dominated by their valence quarks often provides surprisingly good results. This has been pointed out for particle spectra and ratios [30,10,31] and for elliptic flow [12–14]. Most of the work so far has stayed on a qualitative level without quantitative predictions. Recombination of D mesons in heavy ion collisions has been investigated in Ref. [32].

We will argue below that the counting of quantum numbers is a good description of the recombination process for

intermediate momenta. The formalism will set the stage to obtain quantitative results in this regime by recombining quarks from a possibly thermalized phase. We know that the parton phase will not behave like a perturbative plasma near the hadronization point [33]. Instead quarks at hadronization will be effective degrees of freedom exhibiting a mass and gluons will disappear as dynamical degrees of freedom. We will assume here that the effective quarks behave like constituent quarks and that there are no dynamical gluons.

This is different from the work of Greco *et al.* [11] who suggested to recombine one perturbative quark with thermal quarks, leading to an additional contribution at the transition region between the pure thermal phase dominating below 5 GeV/ c and the pure fragmentation regime dominating above 5 GeV/ c . A similar form of this pick-up reaction of a perturbative parton was recently proposed in the context of the sphaleron model [34].

One can also attempt to extend the recombination concept to low P_T , however, the theoretical situation is much more ambiguous there. The main reasons are that the simple counting of quantum numbers violates energy and entropy conservation at low P_T , where the bulk of the hadron yield resides. Nevertheless, once recombination is recognized to be the dominant hadronization mechanism at intermediate P_T from 2 to 5 GeV/ c , it is quite reasonable to expect that this mechanism extends down to very small transverse momentum, where quarks are even more abundant. However, the theoretical description will only be on solid ground once the problems of energy and entropy conservation are addressed properly.

D. A nonrelativistic model

For a first estimate, let us consider a simple static model for the recombination process. We start with a system of quarks and antiquarks which are homogeneously distributed in a fixed three-dimensional volume V with phase-space distributions $w(\mathbf{p})$, so that the number of quarks or antiquarks with a particular set a of quantum numbers (color, spin, isospin) is

$$N_a = V \int \frac{d^3p}{(2\pi)^3} w_a(\mathbf{p}). \quad (3)$$

Hadronization is assumed to occur instantaneously throughout the volume. The distributions $w(\mathbf{p})$ are supposed not to change during the hadronization process, i.e., the quarks are assumed to be quasifree.

The spatial wave functions for a two-particle quark-antiquark state with momenta \mathbf{p}_1 and \mathbf{p}_2 and a meson bound state with momentum \mathbf{P} are

$$\langle x|q, \mathbf{p}_1\mathbf{p}_2\rangle = V^{-1} e^{i(\mathbf{p}_1\mathbf{x}_1 + \mathbf{p}_2\mathbf{x}_2)}, \quad (4)$$

$$\langle x|M, \mathbf{P}\rangle = V^{-1/2} e^{i\mathbf{P}\cdot\mathbf{R}} \varphi_M(\mathbf{y}), \quad (5)$$

respectively, with the center of mass and relative coordinates $\mathbf{R} = (\mathbf{x}_1 + \mathbf{x}_2)/2$ and $\mathbf{y} = \mathbf{x}_1 - \mathbf{x}_2$ for the two quarks in the meson system. To keep our notation simple we omit the proper antisymmetrization of multifermion states, since all

combinatorial factors will cancel in the final result. The internal meson wave function is normalized as

$$\int d^3y |\varphi_M(\mathbf{y})|^2 = 1. \quad (6)$$

The overlap amplitude is given by

$$\langle q, \mathbf{p}_1 \mathbf{p}_2 | M, \mathbf{P} \rangle = \frac{(2\pi)^3}{V^{3/2}} \delta^3(\mathbf{P} - \mathbf{p}_1 - \mathbf{p}_2) \hat{\varphi}_M(\mathbf{q}). \quad (7)$$

Here, we have introduced the relative momentum $\mathbf{q} = (\mathbf{p}_1 - \mathbf{p}_2)/2$, conjugate to \mathbf{y} , and $\hat{\varphi}_M(\mathbf{q})$ is the Fourier transformed wave function. The squared amplitude is

$$|\langle q, \mathbf{p}_1 \mathbf{p}_1 | M, \mathbf{P} \rangle|^2 = \frac{(2\pi)^3}{V^2} \delta^3(\mathbf{P} - \mathbf{p}_1 - \mathbf{p}_2) |\hat{\varphi}_M(\mathbf{q})|^2. \quad (8)$$

We conclude that the total number of mesons found in the quark-antiquark distribution is

$$N_M = C_M V^3 \int \frac{d^3P}{(2\pi)^3} \frac{d^3p_1}{(2\pi)^3} \frac{d^3p_2}{(2\pi)^3} \times w(\mathbf{p}_1) w(\mathbf{p}_2) |\langle q, \mathbf{p}_1 \mathbf{p}_1 | M, \mathbf{P} \rangle|^2 \quad (9)$$

with a degeneracy factor C_M . The momentum distribution of the mesons is given by

$$\frac{dN_M}{d^3P} = C_M \frac{V}{(2\pi)^3} \int \frac{d^3q}{(2\pi)^3} w\left(\frac{\mathbf{P}}{2} + \mathbf{q}\right) w\left(\frac{\mathbf{P}}{2} - \mathbf{q}\right) |\hat{\varphi}_M(\mathbf{q})|^2. \quad (10)$$

From the above equation the spectra of mesons can be calculated for given quark distributions. This will require knowledge of φ_M . The wave function has some width Λ_M , and we assume that it drops rapidly for $|\mathbf{q}| > \Lambda_M$. Let us study the kinematic region where $P \gg \Lambda_M$. The integral over the relative momentum \mathbf{q} is dominated by values $|\mathbf{q}| \sim \Lambda_M$ and thus we can assume that $|\mathbf{q}| \ll |\mathbf{P}|$. We apply a Taylor expansion

$$w\left(\frac{\mathbf{P}}{2} + \mathbf{q}\right) w\left(\frac{\mathbf{P}}{2} - \mathbf{q}\right) = w\left(\frac{\mathbf{P}}{2}\right)^2 + \sum_{ij} q_i q_j \left[w\left(\frac{\mathbf{P}}{2}\right) \partial_i \partial_j w\left(\frac{\mathbf{P}}{2}\right) - \partial_i w\left(\frac{\mathbf{P}}{2}\right) \partial_j w\left(\frac{\mathbf{P}}{2}\right) \right] + O(q^3), \quad (11)$$

where the first order term in the expansion vanishes.

From the lowest-order term in the expansion we get a contribution to the meson spectrum which is independent of the shape of the wave function. Only normalization (6) enters and leads to a universal term

$$C_M \frac{V}{(2\pi)^3} w(\mathbf{P}/2)^2. \quad (12)$$

The second order term (like all higher order terms) in the expansion generates a correction depending on the shape of the wave function. For the sake of simplicity, let us assume a Gaussian shape

$$\hat{\varphi}_M(\mathbf{q}) = \mathcal{N}_M e^{-\mathbf{q}^2/2\Lambda_M^2}. \quad (13)$$

The normalization factor is determined by Eq. (6) as $\mathcal{N}_M^2 = (2\sqrt{\pi}/\Lambda_M)^3$. For this example we have the second order correction

$$C_M \frac{V}{(2\pi)^3} \frac{\Lambda_M^2}{2} \{w(\mathbf{P}/2) \Delta w(\mathbf{P}/2) - [\nabla w(\mathbf{P}/2)]^2\}. \quad (14)$$

We want to emphasize once more that in the limit $P \gg \Lambda_M$ the exact shape of the wave function is not important. In a relativistic framework this statement is softened by the fact that we consider the hadron formation in a boosted frame, where P is large. Therefore Λ_M , which is of the order of Λ_{QCD} in the rest frame of the hadron, will be dilated.

As an example, let us assume an exponential parton distribution of the form $w(\mathbf{p}) = e^{-p/T}$. The meson spectrum at large P is then given by

$$\frac{dN_M}{d^3P} = C_M \frac{V}{(2\pi)^3} e^{-P/T} \left[1 - \frac{2\Lambda_M^2}{TP} \right], \quad (15)$$

using Eqs. (12) and (14). The second order term introduces a power correction of order Λ_M^2/TP to the universal result, depending both on the width of the wave function and the slope of the parton distribution.

For nucleons we start with three quarks at coordinates \mathbf{x}_i . We introduce center of mass and relative coordinates $\mathbf{R} = (\mathbf{x}_1 + \mathbf{x}_2 + \mathbf{x}_3)/3$, $\mathbf{y} = (\mathbf{x}_1 + \mathbf{x}_2)/2 - \mathbf{x}_3$, and $\mathbf{z} = \mathbf{x}_1 - \mathbf{x}_2$.

The overlap amplitude between a three quark state and a baryon with momentum \mathbf{P} is

$$\langle q, \mathbf{p}_1 \mathbf{p}_2 \mathbf{p}_3 | B, \mathbf{P} \rangle = \frac{(2\pi)^3}{V^2} \delta^3(\mathbf{P} - \mathbf{p}_1 - \mathbf{p}_2 - \mathbf{p}_3) \hat{\varphi}_B(\mathbf{q}, \mathbf{s}). \quad (16)$$

Here $\hat{\varphi}_B(\mathbf{q}, \mathbf{s})$ is the baryon wave function in momentum space, depending on the relative momenta \mathbf{q} and \mathbf{s} conjugate to \mathbf{y} and \mathbf{z} , respectively.

Hence the baryon distribution is given by

$$\frac{dN_B}{d^3P} = C_B \frac{V}{(2\pi)^3} \int \frac{d^3q}{(2\pi)^3} \frac{d^3s}{(2\pi)^3} |\hat{\varphi}_B(\mathbf{q}, \mathbf{s})|^2 \times w\left(\frac{\mathbf{P}}{3} + \frac{\mathbf{q}}{2} + \mathbf{s}\right) w\left(\frac{\mathbf{P}}{3} + \frac{\mathbf{q}}{2} - \mathbf{s}\right) w\left(\frac{\mathbf{P}}{3} - \mathbf{q}\right). \quad (17)$$

C_B is the appropriate degeneracy factor. In the region where the nucleon momentum \mathbf{P} is large compared to the intrinsic width of the wave function, we can again expand the product of the quark distribution functions. The leading term is universal and contributes

$$C_B \frac{V}{(2\pi)^3} w(\mathbf{P}/3)^3 \quad (18)$$

to the nucleon distribution. The second order term provides a correction

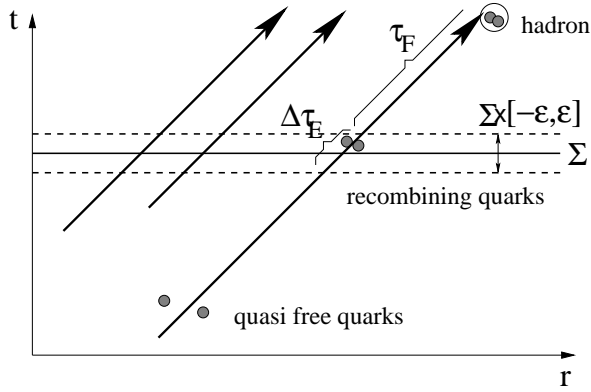


FIG. 1. Sketch of trajectories of hadrons and their precursors moving close to the speed of light in the t - r plane where t is the time in the lab frame and r the radial coordinate. The hypersurface Σ (solid line) and a generalization with finite width (the shell given by dashed lines) are shown. The emission time $\Delta\tau_E$ during which recombination occurs is given by the conditions in the surrounding medium and the trajectory. We approximate this short time by taking the hypersurface Σ infinitely thin. A radially expanding hypersurface does not alter the argument.

$$C_B \frac{V}{(2\pi)^3} \frac{1}{2} \left(\Lambda_{B2}^2 + \frac{3}{4} \Lambda_{B1}^2 \right) \{ w(\mathbf{P}/3)^2 \Delta w(\mathbf{P}/3) - w(\mathbf{P}/3) \times [\nabla w(\mathbf{P}/3)]^2 \}, \quad (19)$$

assuming a normalized Gaussian wave function

$$\hat{\phi}_B(\mathbf{q}, \mathbf{s}) = \mathcal{N}_B e^{-\mathbf{q}^2/2\Lambda_{B1}^2} e^{-\mathbf{s}^2/2\Lambda_{B2}^2}. \quad (20)$$

E. First conclusions

Let us summarize and analyze our first results. The transverse spectrum of mesons from recombination is proportional to $C_M w^2(P_T/2)$ whereas fragmentation would generate a distribution proportional to $D(z) \otimes w(P_T/z)$. For an exponential parton spectrum $w = e^{-P_T/T}$ the ratio of recombination to fragmentation is

$$\frac{R}{F} = \frac{C_M}{\langle D \rangle} e^{-(P_T/T)(1-\langle z \rangle)} \quad (21)$$

where $\langle D \rangle$ and $\langle z \rangle < 1$ are average values of the fragmentation function and the scaling variable. Obviously, for large P_T one always gets $R/F > 1$. In other words, recombination always wins over fragmentation at ‘‘high’’ P_T for an exponential parton spectrum. The same is true for baryons as well as mesons.

Now let us consider a parton distribution given by a power law spectrum $w = A(P_T/\mu)^{-\alpha}$ with a scale μ and $\alpha > 0$. Then the ratio of recombination over fragmentation is

$$\frac{R}{F} = \frac{C_M A}{\langle D \rangle} \left(\frac{4}{\langle z \rangle} \right)^\alpha \left(\frac{P_T}{Q} \right)^{-\alpha} \quad (22)$$

and fragmentation ultimately dominates at high P_T . Again, this holds both for mesons and baryons. This implies that fragmentation from an exponential spectrum and recombi-

nation from a power law spectrum are suppressed. We will thus omit these contributions in our work.

One might ask whether these considerations are still valid in the case of more realistic formulation of recombination. It turns out that the basic formulas obtained above are still valid in a relativistic description. Deviations are less than 20% for $P_T > 2$ GeV/ c .

Given an exponential parton spectrum we note that recombination yields a constant baryon-to-meson ratio. The ratio is then only determined by the degeneracy factors

$$\frac{dN_B^R}{dN_M^R} = \frac{C_B}{C_M}. \quad (23)$$

Just counting the hadron degeneracies, the direct p/π^0 ratio (neglecting protons and pions from secondary hadronic decays) would be ~ 2 , in contrast to ~ 0.2 from fragmentation in pQCD. We will later see that finite mass effects and superposition with the fragmentation process will bring down the p/π^0 ratio from 2 to approximately 1 in the range between 2 and 4 GeV/ c transverse momentum.

III. THE RECOMBINATION FORMALISM

In this section, we turn to a better description of recombination. This will require a more realistic model of the parton phase including longitudinal and transverse expansion as well as an improved space-time picture.

Let us consider a system of quarks and antiquarks evolving in Minkowski space. We choose a spacelike hypersurface Σ on which recombination of these partons into hadrons occurs. In the simplest scenario, that could be just a slice of Minkowski space with fixed time t_0 , leading back to the case we described in the preceding subsection.

It has been discussed in the literature [35,36], how the freeze-out can be smeared around the hypersurface to account for a finite hadron emission time. However, RHIC experiments suggest a very rapid freeze-out. The measured two-particle correlation functions are consistent with an extremely short emission time in the local rest frame, suggesting a sudden transition after which the individual hadrons interact only rarely [37]. Therefore, we assume here an instantaneous recombination, corresponding to an infinitely thin hypersurface.

The microscopic picture is shown in Fig. 1. Quarks moving out of the hot system cross the phase boundary. The relevant time scale is the hadron emission time $\Delta\tau_E$ given by the evolution of the system and the trajectory of the hadron precursor. $\Delta\tau_E$ is the time that, e.g., a $q\bar{q}$ pair has available to decide whether to recombine into a meson while the system in the vicinity crosses the phase boundary. This has to be compared with the hadron formation time τ_F . The sudden recombination assumption is valid if $\Delta\tau_E/\tau_F \ll 1$. The recombination of valence quarks is then decoupled from the actual hadronization—where the bound states of valence quarks become free hadron states—and further hadronic interactions.

A. Wigner function formalism

Recombination has already been considered before in a covariant form utilizing Wigner functions for the process of

baryons coalescing into light nuclei and clusters in nuclear collisions [38,35]. Here, we will provide a derivation for the recombination of a quark–antiquark pair into a meson. The generalization to a three quark system recombining into a baryon is straightforward.

By introducing the density matrix $\hat{\rho}$ for the system of partons, the number of quark–antiquark states that we will interpret as mesons is given by

$$N_M = \sum_{ab} \int \frac{d^3 P}{(2\pi)^3} \langle M; \mathbf{P} | \hat{\rho}_{ab} | M; \mathbf{P} \rangle. \quad (24)$$

Here $|M; \mathbf{P}\rangle$ is a meson state with momentum \mathbf{P} and the sum is over all combinations of quantum numbers—flavor, helicity, and color—of valence partons that contribute to the given meson M . We insert complete sets of coordinates

$$N_M = \int \frac{d^3 P}{(2\pi)^3} d^3 \hat{r}_1 d^3 \hat{r}'_1 d^3 \hat{r}_2 d^3 \hat{r}'_2 \langle M; \mathbf{P} | \hat{r}_1, \hat{r}_2 \rangle \langle \hat{r}_1, \hat{r}_2 | \hat{\rho} | \hat{r}'_1, \hat{r}'_2 \rangle \times \langle \hat{r}'_1, \hat{r}'_2 | M; \mathbf{P} \rangle$$

and change the variables to $\mathbf{r}_{1,2} = (\mathbf{r}_{1,2} + \mathbf{r}'_{1,2})/2$ and $\mathbf{r}'_{1,2} = \mathbf{r}_{1,2} - \mathbf{r}'_{1,2}$. We define the two-parton Wigner function $W_{ab}(\mathbf{r}_1, \mathbf{r}_2; \mathbf{p}_1, \mathbf{p}_2)$ as

$$\left\langle \mathbf{r}_1 - \frac{\mathbf{r}'_1}{2}, \mathbf{r}_2 - \frac{\mathbf{r}'_2}{2} \left| \hat{\rho} \right| \mathbf{r}_1 + \frac{\mathbf{r}'_1}{2}, \mathbf{r}_2 + \frac{\mathbf{r}'_2}{2} \right\rangle = \int \frac{d^3 p_1}{(2\pi)^3} \frac{d^3 p_2}{(2\pi)^3} e^{-i\mathbf{p}_1 \cdot \mathbf{r}'_1} e^{-i\mathbf{p}_2 \cdot \mathbf{r}'_2} W_{ab}(\mathbf{r}_1, \mathbf{r}_2; \mathbf{p}_1, \mathbf{p}_2)$$

and introduce a notation for the meson wave function φ_M ,

$$\left\langle \mathbf{r}_1 + \frac{\mathbf{r}'_1}{2}, \mathbf{r}_2 + \frac{\mathbf{r}'_2}{2} \left| \pi; \mathbf{P} \right. \right\rangle = e^{-i\mathbf{P} \cdot (\mathbf{R} + \mathbf{R}'/2)} \varphi_M \left(\mathbf{r} - \frac{\mathbf{r}'}{2} \right). \quad (27)$$

It is convenient to change coordinates again to

$$\mathbf{R}^{(\prime)} = (\mathbf{r}_1^{(\prime)} + \mathbf{r}_2^{(\prime)})/2, \quad (28)$$

$$\mathbf{r}^{(\prime)} = \mathbf{r}_1^{(\prime)} - \mathbf{r}_2^{(\prime)} \quad (29)$$

with conjugated momenta

$$\tilde{\mathbf{P}} = \mathbf{p}_1 + \mathbf{p}_2, \quad (30)$$

$$\mathbf{q} = (\mathbf{p}_1 - \mathbf{p}_2)/2. \quad (31)$$

We arrive at

$$N_M = \sum_{ab} \int \frac{d^3 P}{(2\pi)^3} \frac{d^3 q}{(2\pi)^3} \int d^3 R d^3 r d^3 r' \times W_{ab} \left(\mathbf{R} + \frac{\mathbf{r}}{2}, \mathbf{R} - \frac{\mathbf{r}}{2}; \frac{\mathbf{P}}{2} + \mathbf{q}, \frac{\mathbf{P}}{2} - \mathbf{q} \right) \times e^{i\mathbf{q} \cdot \mathbf{r}'} \varphi_M \left(\mathbf{r} + \frac{\mathbf{r}'}{2} \right) \varphi_M^* \left(\mathbf{r} - \frac{\mathbf{r}'}{2} \right). \quad (32)$$

The integration over \mathbf{R}' has been carried out and provides the three-momentum conservation $\mathbf{P} = \tilde{\mathbf{P}}$.

We define the Wigner function Φ_M^W of the meson as

$$\Phi_M^W(\mathbf{r}, \mathbf{q}) = \int d^3 r' e^{-i\mathbf{q} \cdot \mathbf{r}'} \varphi_M \left(\mathbf{r} + \frac{\mathbf{r}'}{2} \right) \varphi_M^* \left(\mathbf{r} - \frac{\mathbf{r}'}{2} \right). \quad (33)$$

Then

$$\frac{dN_M}{d^3 P} = (2\pi)^{-3} \sum_{ab} \int d^3 R \int \frac{d^3 q d^3 r}{(2\pi)^3} \times W_{ab} \left(\mathbf{R} + \frac{\mathbf{r}}{2}, \mathbf{R} - \frac{\mathbf{r}}{2}; \frac{\mathbf{P}}{2} + \mathbf{q}, \frac{\mathbf{P}}{2} - \mathbf{q} \right) \Phi_M^W(\mathbf{r}, \mathbf{q}). \quad (34)$$

To evaluate this expression, we have to model the Wigner functions of the parton system and of the meson. We assume that the two-parton Wigner function can be factorized into a product of classical one-particle phase-space distributions w . Furthermore the color and helicity states for each flavor will be degenerate. We can therefore replace the sum over quantum numbers a and b by a degeneracy factor C_M .

We introduce the following simplifications: the spatial width $\Delta \mathbf{r}$ of the hadron wave function, translating into a width of Φ_M^W , will be small compared to the size of the system at hadronization. The phase-space distributions $w(\mathbf{r}; \mathbf{p})$ are steeply falling functions of the momentum \mathbf{p} , but vary much less with the spatial coordinate \mathbf{r} within the typical size $\Delta \mathbf{r}$ of a hadron. We shall assume that the spatial variation of the phase-space distribution is small on this scale, replacing $\mathbf{R} \pm \mathbf{r}/2$ with \mathbf{R} .

In our derivation we implicitly chose an equal time formalism by introducing the spatial coordinate states $|\mathbf{r}\rangle$ at a fixed time. However, in our result the integration over the final-state phase space

$$d^3 P d^3 R = d^3 P d^3 R P \cdot u(R)/E \quad (35)$$

is manifestly Lorentz invariant. Here E is the energy of the four-vector P and $u(R)$ is the future oriented unit vector orthogonal to the hypersurface defined by the hadronization volume. This form can be easily generalized for an arbitrary hadronization hypersurface Σ [39,35]. We have

$$E \frac{dN_M}{d^3 P} = C_M \int_{\Sigma} \frac{d^3 R P \cdot u(R)}{(2\pi)^3} \int \frac{d^3 q}{(2\pi)^3} \times w_a \left(\mathbf{R}; \frac{\mathbf{P}}{2} - \mathbf{q} \right) \Phi_M^W(\mathbf{q}) w_b \left(\mathbf{R}; \frac{\mathbf{P}}{2} + \mathbf{q} \right). \quad (36)$$

a, b now only denote the flavors of the valence quarks in meson M and

$$\Phi_M^W(\mathbf{q}) = \int d^3 r \Phi_M^W(\mathbf{r}, \mathbf{q}) \quad (37)$$

is the spatially integrated Wigner function of the meson.

B. Local light cone coordinates

The structure of hadrons is best known in the infinite momentum frame which is described in light cone coordinates. If we let the hadron momentum \mathbf{P} define the z axis of the hadron light cone (HLC) frame, we can introduce the light cone coordinates, e.g., q^+, q_\perp for the relative momentum q . Note that we denote transverse momenta in the HLC frame—i.e., the component orthogonal to \mathbf{P} —by the label \perp , but transverse momenta in the center of mass (CM) frame of the heavy ion collision—orthogonal to the beam axis—by the label T . The labels $+$ and $-$ always refer to light cone coordinates in the HLC frame for a given \mathbf{P} . We fix the HLC frame by a simple rotation from the CM frame, i.e., $P_+ = (E + |\mathbf{P}|)/\sqrt{2}$. We reintroduce the momentum $k = P/2 - q$ of parton a in the meson. Assuming a mass shell condition $k^2 = m_a^2$ with arbitrary but fixed virtuality m_a , we can rewrite the integral

$$d^3k = d^4k 2k^0 \delta(k^2 - m_a^2) = dk^+ d^2k_\perp \frac{k^0}{k^+} \quad (38)$$

in HLC coordinates. m_a will be of order Λ_{QCD} , or more precisely, of the order of a constituent quark mass. In the HLC frame, where we assume that formally $P^+ \rightarrow \infty$, we parametrize $k^+ = xP^+$ with $0 \leq x \leq 1$. Since $k^- \ll k^+$, we have $k^0/k^+ \approx 1/\sqrt{2}$. We end up with

$$E \frac{dN_M}{d^3P} = C_M \int_\Sigma \frac{d^3R P u(R)}{(2\pi)^3} \int \frac{dx P^+ d^2k_\perp}{\sqrt{2}(2\pi)^3} w_a(R; xP^+, \mathbf{k}_\perp) \times \Phi_M(x, \mathbf{k}_\perp) w_b[R; (1-x)P^+, -\mathbf{k}_\perp]. \quad (39)$$

Here we have rewritten the spatially integrated Wigner function of the meson in terms of light cone coordinates for quark a and approximate it by a squared light cone wave function of the meson

$$\Phi_M(x, \mathbf{k}_\perp) = |\bar{\phi}_M(x, \mathbf{k}_\perp)|^2. \quad (40)$$

The light cone wave functions we introduce here do not necessarily coincide with the light cone wave functions $\Phi_{\text{LC}}(x, \mathbf{k}_\perp, \mu)$ used for exclusive processes in QCD [40]. There, a hadron is decomposed into a series of Fock states of perturbative partons, starting from the valence structure. In terms of this expansion we know that the valence Fock state has only a small contribution at scales $\mu > 1$ GeV. μ is given by the momentum transfer in the hard reaction which is described by pQCD. However, because the momentum transfer in a hard exclusive reaction has to be spread over all partons in the hadron state, the exclusive process itself acts like a filter, weighting the lower Fock states more strongly. In other words, the contributions of higher Fock states, though more likely in the wave function, are generally suppressed by inverse powers of the momentum transfer (higher twist). This usually permits a fairly good description of hard exclusive processes in terms of the lowest Fock state.

As we will discuss below, we expect the parton spectrum of a heavy ion collision at freeze out to be composed of an exponential part at small transverse momentum and a power

law tail, given by pQCD, at high transverse momentum. We will study recombination in the pQCD domain in a forthcoming publication.

Here, we want to focus on recombination from the exponential part of the parton spectrum. It will be given by a slope $1/T^*$ with a temperaturelike parameter T^* . T^* also sets the scale for the typical momentum transfer in the parton medium before hadronization. If T^* is an effective blue shifted temperature $T^* = \sqrt{(1+\beta)/(1-\beta)}T$ in an expanding medium with physical temperature T and flow velocity β , then the typical scale $T < T^*$ will even be smaller. Here we use the phase transition temperature at zero baryon density $T \approx 175$ MeV [41].

We cannot expect that perturbative QCD will work as a description of partons at the phase transition [33]. What are the quanta that recombine? We know that in pQCD for decreasing scales the nonperturbative (long-range) matrix elements describing hadrons get more “valencelike,” though we cannot seriously extend this study to scales below 1 GeV. We will assume here that we recombine effective constituent partons, taking into account only the valence structure of the hadron. Gluons are no dynamic degrees of freedom in this picture, and the quarks and antiquarks will have an effective mass.

This picture is supported by the recent discovery of “magical factors” of 2 and 3 in measurements of spectra and the elliptic flow of mesons and baryons, respectively, at RHIC [16]. Later we will apply our assumptions to partons in the exponential spectrum having as much as 2 GeV/ c of transverse momentum. This might raise doubts about the validity of an effective description. However, we have to keep in mind that the momentum is in principle meaningless, only the momentum transfer experienced by a particle in a reaction sets the scale at which we resolve its structure.

From the normalization condition

$$\langle M; \mathbf{P} | M; \mathbf{P}' \rangle = (2\pi)^3 \delta^3(\mathbf{P} - \mathbf{P}') \quad (41)$$

we infer $\int d^3r \varphi_M(r) = 1$ and finally

$$\int \frac{dk^+ d^2k_\perp}{\sqrt{2}(2\pi)^3} |\bar{\phi}_M(x, \mathbf{k}_\perp)|^2 = 1. \quad (42)$$

This is different from the light cone wave functions in exclusive processes which involve a dimensional quantity connected to the weight of the Fock state, e.g., the pion decay constant f_π in case of the pion.

We further utilize the fact that we work in a kinematic regime where P^+ is large compared to all nonperturbative quantities. Of course, our main concern here is that we do not really know the shape of the wave function ϕ_M . We can choose a factorized ansatz

$$\bar{\phi}_M(x, k_\perp) = \phi_M(x) \Omega(k_\perp) \quad (43)$$

with a longitudinal distribution amplitude $\phi_M(x)$ and a transverse part. We know that the transverse shape should be quite narrow, e.g., given by a Gaussian with a width $\Lambda_\perp \ll P^+$. Considering hadrons at midrapidity, \mathbf{k}_\perp will mainly be pointing in the longitudinal and azimuthal directions in the CM frame, where the variation of the par-

ton distributions w is small. This implies $w(R; xP^+, \mathbf{k}_\perp) \approx w(R; xP^+)$ for typical transverse momenta $\mathbf{k}_\perp \sim \Lambda_{\text{QCD}} \ll P^+$. We can then integrate the \mathbf{k}_\perp dependence of the wave function. This leaves us with

$$E \frac{dN_M}{d^3P} = C_M \int_\Sigma \frac{d^3RP \cdot u(R)}{(2\pi)^3} \int_0^1 dx w_a(R; xP^+) |\phi_M(x)|^2 \times w_b[R; (1-x)P^+]. \quad (44)$$

The amplitude $\phi_M(x)$ encodes the remaining QCD dynamics. We expect it to be peaked around $x=1/2$, meaning that the two quarks will carry roughly the same amount of momentum. But the width of the distribution, since it is formulated in terms of momentum fractions, could be quite broad in momentum space. Thus we cannot use the same argument as for the transverse coordinates in order to integrate out this degree of freedom. However, for an exponential parton spectrum we have

$$w_a(R; xP^+) w_b[R; (1-x)P^+] \sim e^{-xP^+/T} e^{-(1-x)P^+/T} = e^{-P^+/T}. \quad (45)$$

Hence the product of parton distributions is independent of x and we can perform the integral over x , which just gives the trivial normalization of the wave function from Eq. (42) [10]. There will be corrections to that from momentum components other than P^+ which are not additive because energy is not conserved (see the following subsection). Where we want to take into account wave functions, we adopt the asymptotic form of the perturbative pion distribution amplitude

$$\phi_M(x) = \sqrt{30}x(1-x) \quad (46)$$

as a model for mesons.

C. Energy conservation

Energy conservation is not manifest in the recombination approach. Since we are dealing with a $2 \rightarrow 1$ process, one of the particles in general needs to be off mass shell [35]. This does not pose a problem in the physical environment where recombination takes place. Both in the quark phase and in the hadronic phase we expect interactions with the surrounding medium to occur. Since recombination, as described in this work, has been simplified to a counting of quantum numbers and momenta, without real QCD dynamics, we neglect effects of these additional interactions that ensure energy conservation. This is tolerable due to the small time scale of hadronization and that changes in the parton distributions w by interactions during this time are negligible. We also neglect effects that final-state interactions between the hadrons could have on the spectra—these are expected to contribute mainly in the low momentum domain, $P_T < 1$ GeV.

For large momenta \mathbf{P} , the energies of the particles are dominated by the kinetic energies and not by the masses. The light cone wave functions have a transverse width Λ_\perp which is a nonperturbative momentum scale. Therefore the momenta of the recombining quarks will be collinear up to

transverse momenta of order Λ_\perp . This implies that the energy is conserved up to terms of order Λ_\perp^2/P^+ and m^2/P^+ , where m stands for the masses of the participating particles.

Energy conservation is a problem at low transverse momentum and can only be overcome if one takes further interactions between the partons into account. This would require a much more sophisticated formulation that includes nonperturbative initial- and final-state effects.

Restricting ourselves to large transverse momentum finally permits to use light cone fractions x for the spatial momentum \mathbf{P} in the CM frame instead of the momentum P^+ in the HLC frame. The relation $p^+ = xP^+$ between the quark momentum p and the hadron momentum P in light cone coordinates translates to

$$\mathbf{p} = x\mathbf{P} + O\left(x \frac{M^2}{|\mathbf{P}|}\right) + O(\Lambda_\perp). \quad (47)$$

This is a leading order expansion in M^2/\mathbf{P}^2 where M is the hadron momentum. At midrapidity this further translates to the simple formula $p_T = xP_T$ for the transverse momenta.

D. Low transverse momentum and hadron thermodynamics

It is well known that total hadron yields at RHIC can be described very accurately by a purely statistical model, using only hadronic properties, such as masses, chemical potentials, and spin degeneracies [42–44]. The hadron yields are given by the P_T -integrated spectra and are naturally dominated by particles with less than 2 GeV/ c transverse momentum. The picture of thermal hadron production does not necessarily require the existence of a parton phase.

However, one can show that recombination of a thermalized parton phase is consistent with thermal hadron production in the limit $P_T \rightarrow \infty$. Although pQCD will eventually dominate over both mechanisms at large P_T , this nevertheless suggests that the recombination mechanism connects a thermal parton phase with the observed thermal hadron phase. Therefore it is justified to call recombination from a thermal parton phase the microscopic manifestation of statistical hadron production.

E. Summary of the formalism

We want to summarize what we have so far. From Eq. (44) the meson spectrum is given by

$$E \frac{N_M}{d^3P} = C_M \int_\Sigma d\sigma_R \frac{P \cdot u(R)}{(2\pi)^3} \int_0^1 dx w_a(R; x\mathbf{P}) |\phi_M(x)|^2 \times w_b[R; (1-x)\mathbf{P}], \quad (48)$$

where $d\sigma_R$ measures the volume of the hypersurface Σ and $R \in \Sigma$. For baryons, the same steps result in the expression

$$E \frac{N_B}{d^3P} = C_B \int_\Sigma d\sigma_R \frac{P \cdot u(R)}{(2\pi)^3} \int \mathcal{D}x_i w_a(R; x_1\mathbf{P}) \times w_b(R; x_2\mathbf{P}) w_c(R; x_3\mathbf{P}) |\phi_B(x_1, x_2, x_3)|^2. \quad (49)$$

a , b , and c are the valence partons and $\phi_B(x_1, x_2, x_3)$ is the

effective wave function of the baryon in light cone coordinates. We use the short notation

$$\int \mathcal{D}x_i = \int_0^1 dx_1 dx_2 dx_3 \delta(x_1 + x_2 + x_3 - 1) \quad (50)$$

for the integration over three light cone fractions. Inspired by the asymptotic form of the light cone distribution amplitudes for pions and nucleons we choose

$$\phi_M(x) = \sqrt{30}x(1-x), \quad (51)$$

$$\phi_B(x_1, x_2, x_3) = 12\sqrt{35}x_1x_2x_3 \quad (52)$$

for mesons and baryons, respectively.

These wave functions are broad in momentum space. In order to study the effect of the width of the wave functions on our results it will be interesting to alternatively explore the case of narrow wave functions in the spirit of Sec. II D. The limiting case are δ -shaped wave functions

$$|\phi_M(x)|^2 = \delta(x - \frac{1}{2}) \quad (53)$$

$$|\phi_B(x_1, x_2, x_3)|^2 = \delta(x_1 - \frac{1}{3})\delta(x_2 - \frac{1}{3}). \quad (54)$$

The spectra are then given by

$$E \frac{N_M}{d^3P} = C_M \int_{\Sigma} d\sigma_R \frac{P \cdot u(R)}{(2\pi)^3} w_a\left(R; \frac{\mathbf{P}}{2}\right) w_b\left(R; \frac{\mathbf{P}}{2}\right), \quad (55)$$

$$E \frac{N_B}{d^3P} = C_B \int_{\Sigma} d\sigma_R \frac{P \cdot u(R)}{(2\pi)^3} w_a\left(R; \frac{\mathbf{P}}{3}\right) w_b\left(R; \frac{\mathbf{P}}{3}\right) w_c\left(R; \frac{\mathbf{P}}{3}\right). \quad (56)$$

It is an important observation that in the case of exponential parton distributions, the shape of the wave function is almost negligible. We have to be aware that there will be corrections to the above equations of order $m/|\mathbf{P}|$ and $\Lambda_{\text{QCD}}/|\mathbf{P}|$, where m is the mass of the hadron or the partons, reducing their range of applicability to large \mathbf{P} .

On the other hand, the spectrum of hadrons from fragmentation is given by Eq. (1),

$$E \frac{dN_h}{d^3P} = \sum_a \int_0^1 \frac{dz}{z^2} D_{a \rightarrow h}(z) E_a \frac{dN_a}{d^3P_a}. \quad (57)$$

The number of partons can be obtained from the cross section via the impact parameter dependent nuclear thickness function $dN/d^3P = T_{\text{AuAu}}(b) d\sigma/d^3P$. We take $T_{\text{AuAu}}(0) = 9A^2/8\pi R_A^2$ for central collisions. $R_A = A^{1/3}1.2$ fm is the radius of the nucleus.

IV. HADRONS AND PARTON SPECTRA

In the following we want to discuss the parton phase created in collisions of gold nuclei at RHIC with $\sqrt{s} = 200$ GeV per nucleon pair. We will then proceed to calculate the hadron spectra emerging from recombination and fragmentation of this parton phase.

A. Modeling the parton phase

Assuming longitudinal boost invariance, we fix the hypersurface Σ by choosing $\tau = \sqrt{t^2 - z^2} = \text{const}$ for

$$R^\mu = (t, x, y, z) = (\tau \cosh \eta, \rho \cos \phi, \rho \sin \phi, \tau \sinh \eta). \quad (58)$$

It is convenient to introduce the space-time rapidity η and the radial coordinate ρ , since the measure for the hypersurface Σ then takes the simple form $d\sigma_R = \tau d\eta \rho d\rho d\phi$ and the normal vector is given by

$$u^\mu(R) = (\cosh \eta, 0, 0, \sinh \eta). \quad (59)$$

Using a similar parametrization of the parton momentum

$$p^\mu = (m_T \cosh y, p_T \cos \Phi, p_T \sin \Phi, m_T \sinh y) \quad (60)$$

with rapidity y and transverse mass $m_T = \sqrt{m^2 + p_T^2}$, we obtain $p \cdot u(R) = m_T \cosh(\eta - y)$. We remind the reader that we will use capitalized variables (P, P_T, M, M_T , etc.) for hadrons.

Now we have to specify the spectrum of partons. As already discussed above we assume that the parton spectrum consists of two domains. At large p_T , the distribution of partons is given by perturbative QCD and follows a power law. For the transverse momentum distribution at midrapidity for central collisions ($b=0$) we use the parametrization [45,46]

$$\left. \frac{dN_a^{\text{pert}}}{d^2p_T dy} \right|_{y=0} = K \frac{C}{(1 + p_T/B)^\beta}. \quad (61)$$

The parameters C , B , and β are taken from a leading order (LO) pQCD calculation and can be found in Ref. [46] for the three light quark flavors and gluons. A constant K factor of 1.5 is included to roughly account for higher order corrections in α_s [47]. The calculation includes nuclear shadowing of the parton distributions, but no higher twist initial-state effects. Higher twist effects, such as the Cronin effect, will fade like $A^{1/3} \Lambda_{\text{QCD}}^2 / P_T^2$ for high transverse momentum [48]. Since we will show that fragmentation and pQCD are only dominant for transverse momenta above 5 GeV/c in the hadron spectrum for RHIC, it is safe to omit the Cronin effect.

Energy loss of partons, resulting in a shift of the transverse momentum spectrum [3,4], is taken into account and parametrized as

$$\Delta p_T(b, p_T) = \epsilon(b) \sqrt{p_T} \frac{\langle L \rangle}{R_A}. \quad (62)$$

For collisions at impact parameter $b=0$ we take $\langle L \rangle = R_A$ and therefore $\Delta p_T(0, p_T) = \epsilon(0) \sqrt{p_T}$ (we postpone the discussion of the impact parameter dependence to Sec. IV C). The choice of $\langle L \rangle = R_A$ neglects the fact that for the strong quenching observed at RHIC energies, jet emission becomes a surface effect [4,49]. However, we note that only the product $\epsilon \langle L \rangle$ as a whole is a parameter. We have no ambition here to make a connection to the microscopic parameters of jet quenching, therefore we will not disentangle ϵ and $\langle L \rangle$. This would require a more sophisticated

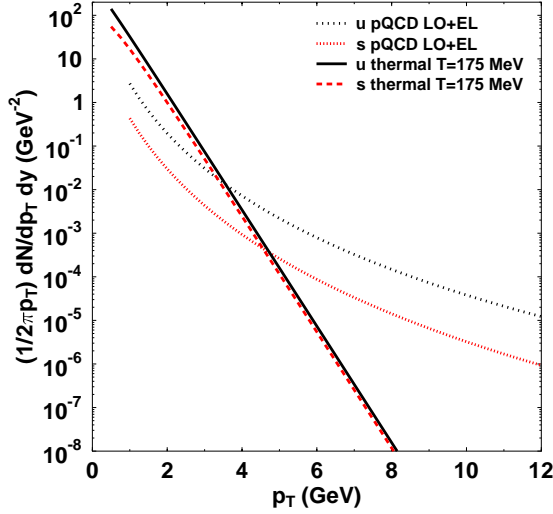


FIG. 2. (Color online) Spectrum of u and s quarks at hadronization in a central Au+Au collision at RHIC. Perturbative partons from hard QCD processes with subsequent energy loss (dashed lines) and the thermal phase with $T=175$ MeV and radial flow $v_T=0.55c$ (solid lines) are shown.

model of the emission geometry. We also do not use a radial profile for the emission and the density of the medium. This can be found discussed elsewhere in the literature [4,21,22]. Nevertheless, our “minimal” description of

energy loss is quite successful to describe the available data on high- P_T spectra ($P_T > 5$ GeV/ c) for π^0 , K_s^0 , and charged hadrons $(h^+ + h^-)/2$ in central Au+Au collisions. From a fit to these data we find $\epsilon_0 = \epsilon(0) = 0.82$ GeV $^{1/2}$ for central Au+Au collisions. This value corresponds to an average energy loss of 3 GeV for a 10 GeV parton in a Au+Au collision with $b=0$. The perturbative spectrum for up and strange quarks at midrapidity is shown in Fig. 2. For fragmentation of pions, kaons, protons, and antiprotons we use LO KKP fragmentation functions with the scale set to the hadron transverse momentum P_T [19]. Λ fragmentation is calculated with the LO fragmentation functions of de Florian, Stratmann, and Vogelsang [50].

Besides the perturbative tail of the parton spectrum that will turn into hadrons via fragmentation, we assume the existence of a spectrum of thermalized partons that are recombining at hadronization and dominate at low and intermediate values of p_T . In this phase we assume the effective degrees of freedom to be constituent quarks without dynamical gluons. We take the spectrum to be exponential with a given temperature T ,

$$w_a(R; p) = \gamma_a e^{-p \cdot v(R)/T} e^{-\eta^2/2\Delta^2} f(\rho, \phi). \quad (63)$$

γ_a is a fugacity factor for each parton species a . We also include longitudinal and radial flow through the velocity vector

$$v^\mu(R) = (\cosh \eta_L \cosh \eta_T, \sinh \eta_T \cos \phi, \sinh \eta_T \sin \phi, \sinh \eta_L \cosh \eta_T). \quad (64)$$

$\eta_L(R)$ and $\eta_T(R)$ are the rapidities of the longitudinal and radial flow which still could depend on the space-time point $R \in \Sigma$. For the longitudinal expansion we choose a Bjorken scenario where the longitudinal rapidity is simply fixed by the space-time rapidity

$$\eta_L(R) = \eta. \quad (65)$$

The transverse flow is given by a velocity $v_T(R)$ with $v_T = \tanh \eta_T$. For practical purposes we will not work with a radial profile but assume v_T to be independent of ρ and ϕ . However, for collisions with finite impact parameter b we will later allow a dependence of v_T on the azimuthal angle ϕ in order to describe the measured elliptic asymmetry in the spectra. The space-time structure of the parton source in Eq. (63) is given by a transverse distribution $f(\rho, \phi)$ and a wide Gaussian rapidity distribution with a width Δ .

We assume that hadronization occurs at $\tau=5$ fm at a temperature $T=175$ MeV in the parton phase. This is consistent with predictions of the phase transition temperature at vanishing baryon chemical potential from lattice QCD [41]. For the spread of the parton distribution in longitudinal direction we choose $\Delta=2$. The constituent quark masses are taken to be 260 MeV for u and d quarks and 460 MeV for s quarks.

The two component model of the parton spectrum with an exponential bulk and a power law tail is also predicted by parton cascades like VNI/BMS [51], although the interactions in that case are purely perturbative. This implies that an exponential shape of the spectrum does not necessarily mean that the parton system is in thermal equilibrium.

In the region where contributions from recombination and fragmentation are of the same size we expect other mechanisms to play a role, which interpolate between the two pictures. This could include partial recombination and higher twist fragmentation. In the absence of a consistent description of these mechanisms we simply add both contributions to the hadron spectrum—recombination from the exponential part and the fragmentation from the pQCD part—for $P_T > 2$ GeV/ c .

B. Degeneracy factors

It is not *a priori* clear from QCD what the degeneracy factors C_h for each hadron h are. In principle, every quark has three color and two spin degrees of freedom. One could argue that three quarks of any color and spin can form a proton and that quantum numbers can be “corrected” at no cost by the emission of soft gluons. That would lead to de-

generacy factors $C_p=2 \times (3 \times 2)^3$ and $C_{\pi^0}=(3 \times 2)^2$. On the other hand, there are no dynamical gluons in our picture and it would be consistent to require recombining partons to have the right quantum numbers at the beginning.

Surprisingly this is supported from work on recombination in pQCD, where the contributions from color octets and spin-flip states to the recombination of D mesons were found to be small [26]. Using this assumption, the degeneracies are only determined by the degrees of freedom of the hadron, e.g., $C_p=2$, $C_\pi=1$, etc. These are exactly the degeneracies used in the statistical thermal model. We will not take into account feed-down from decays of resonances, except for the Λ , where the Σ^0 is too close in mass to be suppressed. Hence we use $C_\Lambda=4$.

This is different from Ref. [10] where we counted Δ resonances to give nucleons with weight 1. However, this overestimates the correction from Δ decays. Nevertheless, the degeneracy of 5/3 given in Ref. [10] for the proton was of the right size due to a mistake in the normalization of the baryon states, which gave an additional factor of 1/3!. Therefore the numerical results given in Ref. [10] are still valid.

We should add that due to the small but probably nonvanishing color octet and spin flip contributions and due to feed-down corrections we expect all degeneracy factors to have an error of at least 20%.

C. Central collisions

For the momentum spectrum of quarks

$$E \frac{dN_a^{\text{th}}}{d^3p} = g \gamma_a \int_{\Sigma} d\sigma_R \frac{p \cdot u(R)}{(2\pi)^3} w_a(R; p) \quad (66)$$

we rewrite the exponent in Eq. (63) as

$$p \cdot v(R) = m_T \cosh(\eta - y) \cosh \eta_T - p_T \cos(\phi - \Phi) \sinh \eta_T, \quad (67)$$

where m_T is the transverse mass of quark a . The factor $g=6$ in Eq. (66) is counting the color and spin degeneracies. In the case of central collisions (impact parameter $b=0$) we can assume that v_T and f are independent of ϕ . For simplicity we furthermore assume that f is also independent of the radial coordinate ρ and that the radial distribution of the partons is homogeneous up to a radius ρ_0 : $f(\rho)=\Theta(\rho_0-\rho)$. We can then easily perform the ϕ and ρ integrals in Eq. (66). If we consider the region around $y=0$, we can also neglect the Gaussian profile function in η , since $\eta^2/\Delta^2 \ll (m_T/T) \cosh \eta$, and integrate over this variable analytically.

The transverse momentum spectrum of partons in the thermal phase is then given by

$$\left. \frac{dN_a^{\text{th}}}{d^2p_T dy} \right|_{y=0} = 2g \gamma_a m_T \frac{\tau A_T}{(2\pi)^3} \times I_0 \left[\frac{P_T \sinh \eta_T}{T} \right] K_1 \left[\frac{m_T \cosh \eta_T}{T} \right]. \quad (68)$$

$A_T=\rho_0^2\pi$ is the transverse area of the parton system and I_0

and K_1 are modified Bessel functions. Figure 2 also shows the thermal spectrum of up and strange quarks. The radial flow velocity $v_T=0.55c$, fugacities $\gamma_u=\gamma_d=1$, $\gamma_s=\gamma_{\bar{s}}=0.9$, $\gamma_c=\gamma_{\bar{c}}=0.8$ and the radius $\rho_0=9$ fm were determined by fits of our calculation to the measured hadron spectra in central collisions, see below.

The transverse momentum spectrum of hadrons formed by recombination from the thermal parton spectrum can be derived from Eqs. (48) and (49) to be

$$\left. \frac{dN_M}{d^2P_T dy} \right|_{y=0} = C_M M_T \frac{\tau A_T}{(2\pi)^3} 2 \gamma_a \gamma_b I_0 \left[\frac{P_T \sinh \eta_T}{T} \right] \times \int_0^1 dx |\phi_M(x)|^2 k_M(x, P_T), \quad (69)$$

$$\left. \frac{dN_B}{d^2P_T dy} \right|_{y=0} = C_B M_T \frac{\tau A_T}{(2\pi)^3} 2 \gamma_a \gamma_b \gamma_c I_0 \left[\frac{P_T \sinh \eta_T}{T} \right] \times \int \mathcal{D}x_i |\phi_B(x_1, x_2, x_3)|^2 k_B(x_i, P_T) \quad (70)$$

for mesons and baryons, respectively. We introduced the short notations

$$k_M(x, P_T) = K_1 \left[\frac{\cosh \eta_T}{T} \left[\sqrt{m_a^2 + x^2 P_T^2} + \sqrt{m_b^2 + (1-x)^2 P_T^2} \right] \right], \quad (71)$$

$$k_B(x_i, P_T) = K_1 \left[\frac{\cosh \eta_T}{T} \left[\sqrt{m_a^2 + x_1^2 P_T^2} + \sqrt{m_b^2 + x_2^2 P_T^2} + \sqrt{m_c^2 + x_3^2 P_T^2} \right] \right]. \quad (72)$$

Here m_a , m_b , and m_c are the masses of the valence quarks and M_T is the transverse mass of the hadron. The most central data bin of the experimental collaborations always corresponds to an average impact parameter larger than zero. Therefore we choose $b=3$ fm to compare to data with 0–5 % and 0–10 % centrality. See the following subsection for a discussion of the impact parameter dependence. Figure 3 shows the result of our calculation for the spectra of pions, protons, antiprotons, kaons, lambdas, xis, and omegas for central collisions. See Sec. V for discussion.

D. Peripheral collisions

In order to describe peripheral collisions, we have to scale the perturbative part of the parton spectrum given in Eq. (61) by the ratio of thickness functions, or equivalently by the number of binary nucleon collisions

$$dN_a^{\text{pert}}(b) = \frac{T_{\text{AuAu}}(b)}{T_{\text{AuAu}}(0)} dN_a^{\text{pert}} = \frac{N_{\text{coll}}(b)}{N_{\text{coll}}(0)} dN_a^{\text{pert}}. \quad (73)$$

Our values for the number of collisions N_{coll} as a function of impact parameter are listed in Table I and are close to the values used by PHENIX Collaboration [52].

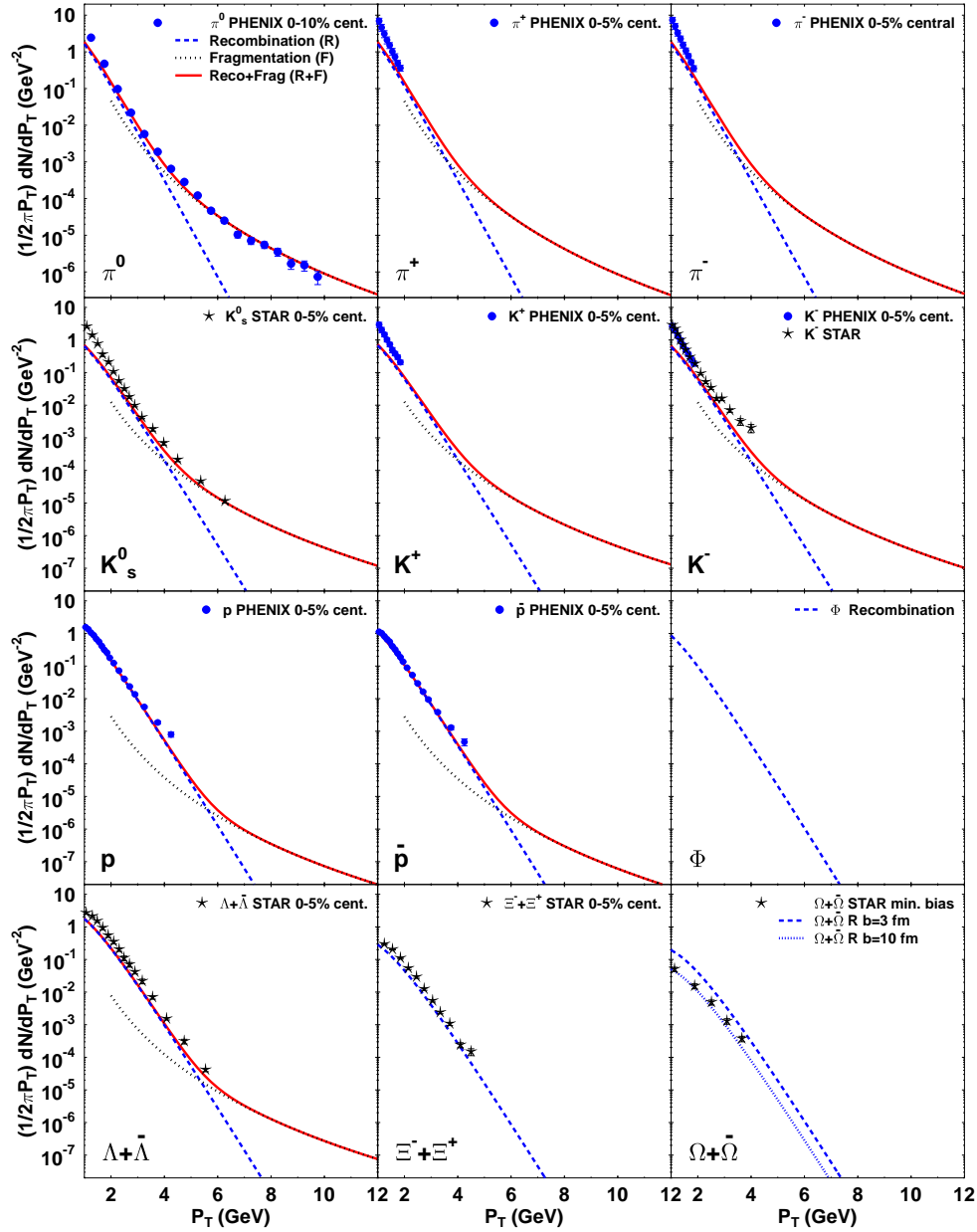


FIG. 3. (Color online) Hadron spectra at midrapidity as a function of transverse momentum P_T for central Au+Au collisions at $\sqrt{S} = 200$ GeV. We show fragmentation (dotted line), recombination (dashed line) and the sum of both contributions (solid line) at $b=3$ fm vs data from PHENIX and STAR (for Φ , $\Xi^+ + \Xi^-$, and $\Omega + \bar{\Omega}$ recombinations only). $\Omega + \bar{\Omega}$ data are minimum bias, therefore the result of a calculation with impact parameter $b=10$ fm is also shown. All data are preliminary except π^0 , p , and \bar{p} data from PHENIX. All error bars give statistical errors only, except for π^0 data from PHENIX which give the total error. See Sec. V for more details.

The length and width of the overlap zone of two nuclei with radius R_A , colliding at impact parameter b , are $l(b) = \sqrt{R_A^2 - (b/2)^2}$ and $w(b) = R_A - b/2$. We scale the average length entering the energy loss in Eq. (62) as $\langle L \rangle = [l(b) + w(b)]/2$. On the other hand, the density of the hot medium is decreasing with increasing impact parameter. We choose the simple ansatz

$$\epsilon(b) = \epsilon_0 \frac{1 - e^{-(2R_A - b)/R_A}}{1 - e^{-2}} \quad (74)$$

for the b dependence of the energy loss parameter, which describes the data surprisingly well. We refer to Ref. [4]

for more detailed studies of the jet quenching effect.

For the thermal phase of the parton spectrum, we keep the temperature T and the hadronization time τ independent of the impact parameter b , but adjust the size of the volume according to the profile function $f(\rho)$. We scale the transverse area A_T of the parton phase at hadronization with the transverse area of the overlap zone of the two nuclei

$$A_T(b) = \frac{l(b)w(b)\pi}{R_A^2\pi} A_T(0) = l(b)w(b) \frac{\rho_0^2}{R_A^2}. \quad (75)$$

In principle, the radial flow velocity v_T is expected to vary with impact parameter. However, it turns out that the

TABLE I. Average number of binary nucleon collisions N_{coll} for some values of the impact parameter b in collisions of gold nuclei.

b (fm)	0	3	5.5	7.5	9	10	11	12	13	13.9
N_{coll}	1146	913	594	350	199	120	61.6	26.0	10.0	5.3

slope of the measured hadron spectra above 2 GeV/ c is consistent with a constant flow velocity $v_T=0.55c$ up to very large impact parameters, so that we fix this value for all b . It may be questionable whether partons are produced in equilibrium in peripheral collisions. We therefore introduce an additional impact parameter dependent fugacity $\gamma(b)$ common to all quark flavors. However, the measured hadron spectra favor $\gamma(b)=1$ up to high values of b . Corrections are only necessary for very peripheral collisions. We take $\gamma(b)=1$ for $b \leq 10.5$ fm, $\gamma(11 \text{ fm})=0.7$, $\gamma(12 \text{ fm})=0.4$, and $\gamma(13 \text{ fm})=0.4$.

E. Elliptic flow

For hadrons from fragmentation we assume that the azimuthal anisotropy in peripheral collisions is induced by the azimuthal dependence of the energy loss [53,54,49,4]. To determine the coefficient v_2 we generalize Eq. (62) to

$$\Delta p_T(b, p_T, \Phi) = \epsilon_0 \sqrt{p_T} \frac{\langle L \rangle}{R_A} (1 - \alpha \cos 2\Phi), \quad (76)$$

where $\epsilon(b)$ is given by Eq. (74). This leads to a spectrum d^2N/dP_T^2 with nontrivial dependence on Φ . From that we obtain the elliptic flow by applying the definition

$$v_2^{\ell}(p_T) = \langle \cos(2\Phi) \rangle = \frac{\int d\phi \cos 2\phi I_2[p_T \sinh \eta_T(\phi)/T] K_1[m_T \cosh \eta_T(\phi)/T]}{\int d\phi I_0[p_T \sinh \eta_T(\phi)/T] K_1[m_T \cosh \eta_T(\phi)/T]}. \quad (81)$$

Our assumptions imply $v_2^{\ell} = v_2^r = v_2^l = v_2^{\bar{l}}$ in the thermal phase, but $v_2^{\ell} = v_2^{\bar{l}}$ differ slightly at small p_T because of the bigger strange quark mass. We determine the parameter p_0 in the parametrization of the parton phase from a comparison to the PHENIX measurement of the elliptic flow of pions [57]. We obtain $p_0=1.1$ GeV/ c .

After having fixed the coefficient $v_2^a(p_T)$ for each parton species a we write the azimuthally anisotropic phase-space distribution for thermal partons at midrapidity as

$$w_a^{\text{ai}}(R; p) = w_a(R; p) [1 + 2v_2^a(p_T) \cos 2\Phi]. \quad (82)$$

Here $w_a(R; p)$ is the phase space distribution without anisotropy from Eq. (63). Substituting this into the basic recombination formulas (48) and (49) we obtain

$$v_2^M(P_T) = \frac{\int dx |\phi_M(x)|^2 \{v_2^a(xP_T) + v_2^b[(1-x)P_T]\} k_M(x, P_T)}{\int dx |\phi_M(x)|^2 \{1 + 2v_2^a(xP_T)v_2^b[(1-x)P_T]\} k_M(x, P_T)}, \quad (83)$$

$$v_2(P_T) = \langle \cos 2\Phi \rangle = \frac{\int d\Phi \cos 2\Phi d^2N/dP_T^2}{\int d\Phi d^2N/dP_T^2}. \quad (77)$$

The parameter α is given by the collision geometry. It has the value

$$\alpha = \frac{w(b) - l(b)}{w(b) + l(b)} \quad (78)$$

for given impact parameter b .

In the thermal phase, the hydrodynamic expansion from an originally anisotropic overlap zone of both nuclei (for $b \neq 0$) induces an elliptic anisotropy of the parton spectrum. This leads to a dependence of the transverse flow on the azimuthal angle ϕ . To model the anisotropy in the parton phase we take the azimuthal dependence of the transverse rapidity to be

$$\eta_T(\phi) = \eta_T^0 [1 - f(p_T) \cos 2\phi]. \quad (79)$$

Here η_T^0 is the rapidity given by the flow velocity $v_T = 0.55c$, so that $\tanh \eta_T^0 = 0.55$. The amplitude of the anisotropy $f(p_T)$ is given by the geometrical anisotropy α at low transverse momenta, but faster partons will experience the anisotropy in the expansion less than slower ones. Therefore we choose an ansatz

$$f(p_T) = \frac{\alpha}{1 + (p_T/p_0)^2}. \quad (80)$$

From Eqs. (66) and (67) one obtains [55,56]

$$v_2^B(P_T) = \frac{\int \mathcal{D}x_i |\phi_B(x_i)|^2 [v_2^a(x_1 P_T) + v_2^b(x_2 P_T) + v_2^c(x_3 P_T) + 3v_2^a(x_1 P_T)v_2^b(x_2 P_T)v_2^c(x_3 P_T)] k_B(x_i, P_T)}{\int \mathcal{D}x_i |\phi_B(x_i)|^2 \{1 + 2[v_2^a(x_1 P_T)v_2^b(x_2 P_T) + v_2^a(x_1 P_T)v_2^c(x_3 P_T) + v_2^b(x_2 P_T)v_2^c(x_3 P_T)]\} k_B(x_i, P_T)} \quad (84)$$

for the anisotropies in the meson and baryon spectra, respectively. Using the δ -function approximation this reduces to the relations already given before in the literature [14,15]

$$v_2^M(P_T) = \frac{v_2^a(\frac{1}{2}P_T) + v_2^b(\frac{1}{2}P_T)}{1 + 2v_2^a(\frac{1}{2}P_T)v_2^b(\frac{1}{2}P_T)}, \quad (85)$$

$$v_2^B(P_T) = \frac{v_2^a(\frac{1}{3}P_T) + v_2^b(\frac{1}{3}P_T) + v_2^c(\frac{1}{3}P_T) + 3v_2^a(\frac{1}{3}P_T)v_2^b(\frac{1}{3}P_T)v_2^c(\frac{1}{3}P_T)}{1 + 2v_2^a(\frac{1}{3}P_T)v_2^b(\frac{1}{3}P_T) + 2v_2^b(\frac{1}{3}P_T)v_2^c(\frac{1}{3}P_T) + 2v_2^c(\frac{1}{3}P_T)v_2^a(\frac{1}{3}P_T)}. \quad (86)$$

If we assume one universal partonic v_2 for the recombining quarks, the above expressions simplify to

$$v_{2,M}(P_T) = \frac{2v_2(\frac{1}{2}P_T)}{1 + 2v_2(\frac{1}{2}P_T)^2}, \quad (87)$$

$$v_{2,B}(P_T) = \frac{3v_2(\frac{1}{3}P_T) + 3v_2(\frac{1}{3}P_T)^3}{1 + 6v_2(\frac{1}{3}P_T)^2}. \quad (88)$$

Since the maximal values of v_2 will be of the order of 0.1, we can neglect the quadratic and cubic terms and arrive at the following simple scaling law, which connects the elliptic flow of hadrons v_2^h to those of the partons v_2 :

$$v_2^h(P_T) = n v_2 \left(\frac{1}{n} P_T \right) \quad (89)$$

with n being the number of valence quarks and antiquarks contained in hadron h . This scaling law was indeed already found to hold in STAR data on the elliptic flow of Λ and K_s^0 down to transverse momenta of about 500 MeV/c [16]. This is a very strong support for the recombination picture. Apparently a part of the uncertainty in the recombination mechanism at low P_T , introduced by the violation of energy conservation, cancels after taking the ratios in Eqs. (83) and (84). The recombination formalism seems to give valid results for v_2 down to transverse momenta of several hundred MeV/c.

We combine the contributions to the anisotropic flow from recombination and fragmentation by using the relative weight $r(P_T)$ for the recombination process

$$v_2(P_T) = r(P_T)v_{2,R}(P_T) + [1 - r(P_T)]v_{2,F}(P_T). \quad (90)$$

$r(P_T)$ is defined as the ratio of the recombination contribution to the spectrum and the total yield,

$$r(P_T) = \frac{dN^R/d^2P_T}{(dN^R/d^2P_T + dN^F/d^2P_T)}. \quad (91)$$

F. The statistical thermal model

In this subsection we give a brief account of the statistical model following variant I of Ref. [42]. For further details we refer the reader to the comprehensive literature [42–44,58].

The hadron spectrum is supposed to emerge from a hypersurface Π and has the form

$$E \frac{dN_h}{d^3P} = \int_{\Pi} d\sigma_R \frac{P \cdot v(R)}{(2\pi)^3} G_h(R; P). \quad (92)$$

We use the same parametrization for the four-velocity $v(R)$ as in Eq. (64). The hypersurface Π is determined by the condition $\sqrt{v^2} = \tau_{SM} = \text{const}$. The hadronic phase-space distribution functions are given by

$$G_h(R; P) = \frac{C_h f_{SM}(r)}{e^{-(Pv - \mu_B B_h - \mu_S S_h - \mu_I I_h)/T_{SM} \pm 1}}, \quad (93)$$

for bosons and fermions, respectively. $r = \tau_{SM} \sinh \eta_T$ is the radial coordinate and $f_{SM}(r) = \Theta(r_0 - r)$ is a radial profile function providing a cylindrical shape. C_h is the degeneracy factor and B_h , S_h , and I_h are baryon number, strangeness, and third component of the isospin for hadron species h .

Equation (92) can be evaluated analogous to Eq. (66). We note that in the limit $P_T \rightarrow \infty$ Eqs. (69) and (70) are equivalent to (92) if the same hypersurface and the same temperature and chemical potentials are used. This is an indication that recombination from a thermal parton phase is the underlying microscopic picture of hadron production in a statistical model. While we will not elaborate on this in more detail, we will quote some results of the statistical model for hadron ratios and compare with our calculation.

The geometric parameters are fixed to be $\tau_{SM} = 7.66$ fm and $r_0 = 6.69$ fm for most central collisions at RHIC in Ref. [42]. Particle ratios at midrapidity in a boost-invariant model are not influenced by the expansion of the system [42], thus we can use the parameters which are determined by particle ratios from the entire phase space. We follow [43] and set $T_{SM} = 177$ MeV, $\mu_B = 29$ MeV, $\mu_S = 10$ MeV, and $\mu_I = -0.5$ MeV.

G. Note on the parameters in our model

We want to give a brief summary of all the parameters for the parton phase. Essentially we have three degrees of freedom for central collisions. These are the energy loss given by $\epsilon_0(L)$, the slope of the exponential part given by temperature T , and radial flow velocity v_T and the normalization of the recombination spectrum by the volume τA_T . In addition there are the parton fugacities. After fixing $\langle L \rangle$, T , and τ to physical or at least reasonable values, we retain ϵ_0 , v_T , and ρ_0 as true parameters that were determined by fitting to the final data given by PHENIX for the inclusive π^0 spectrum [52]. This is in contrast to our previous study where the parameters of the parton spectrum were fixed by the preliminary charged hadron spectrum [10].

The light quark fugacity was set to 1 in accordance with the measured p/π^0 ratio and the fugacities for antiquarks and strange quarks were obtained from other ratios. The ratio of fugacities $\gamma_\pi/\gamma_u=0.9$ can be translated into a baryon chemical potential $\mu_B=27$ MeV. For other impact parameters, the simple geometric scaling of the volume and the number of collisions with b and a reasonable ansatz for $\epsilon(b)$ describe the data up to $b=10$ fm. Only for very peripheral collision there is the need to introduce the new parameter $\gamma(b)$.

V. NUMERICAL RESULTS

In this section we are going to discuss our numerical results on hadron production.

A. Hadron spectra

In Fig. 3 we show our results for hadron production from fragmentation and recombination in central Au+Au collision at $\sqrt{s}=200$ GeV for impact parameter $b=3$ fm. We compare to available experimental data from the PHENIX and STAR Collaborations at RHIC. The π^0 spectrum has been measured by PHENIX up to 10 GeV/c. The final data were released very recently [52] together with final data for neutral pion production in $p+p$ collisions up to 14 GeV/c [59]. Error bars show the total error in the π^0 yield. All our calculations use expressions (48) and (49) with realistic light cone wave functions (51). For protons and neutral pions we also performed the calculations in the δ -function approximation for the wave functions (55) and (56). Figure 4 shows the relative deviation $r_\delta=(dN-dN_\delta)/dN$ of the π^0 and p spectrum in δ -function approximation from the recombination calculation using realistic wave functions. The deviation is less than 22% for protons and less than 12% for pions at small P_T . It becomes considerably smaller at larger P_T since the violation of energy conservation is less important there. This explains why calculations using (55) and (56) are often satisfactory.

Preliminary data on π^+ and π^- production are only available up to 2 GeV/c [60], but we can expect that the global behavior of charged pions is similar to that of neutral pions. All data except for π^0 , p , and \bar{p} shown in Fig. 3 are preliminary. Only statistical errors are given for all sets besides π^0 . In the pion spectra we clearly see the two P_T domains of hadron production. Above 4–5 GeV/c the spectrum is dominated by fragmentation and follows a power law. Below

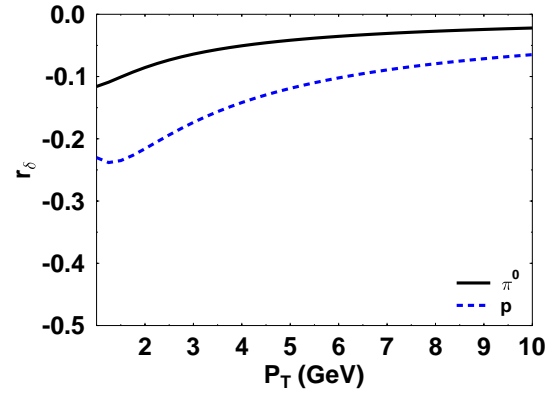


FIG. 4. (Color online) Relative deviation r_δ of the δ -function approximation from calculations using wide wave functions for neutral pions and protons.

4 GeV/c the spectrum is exponential and dominated by recombination from the thermal phase. In our calculation the contribution from fragmentation is artificially cut off below 2 GeV/c (corresponding to a lower cutoff of about 4 GeV/c in the parton spectrum) because perturbative QCD loses its validity at low P_T .

In the crossover region the yield is slightly underestimated, due to our simplified treatment not allowing for recombination involving perturbative partons and mixed mechanisms [11]. We also note that below 2 GeV/c the calculated recombination spectrum bends down and underestimates the data. This effect is caused by neglecting the large binding energy of pions in our recombination formalism, in which pions have an effective mass of $2m_u \approx 520$ MeV compared to the true pion mass of 140 MeV. In addition, pions from secondary decays of hadronic resonances are an important contribution at very low P_T .

The same effect can be seen in the kaon spectra, where we again underestimate the yield for $P_T < 2$ GeV/c. The K_s^0 spectrum was measured by STAR up to 6 GeV/c [61]. The preliminary K^+ and K^- spectra up to 2 GeV/c are available from PHENIX [60], and first results on K^- from STAR up to 4 GeV/c were shown recently [61]. The K_s^0 data above 2 GeV/c can be described very well by our calculations. We note that the last four data points of the preliminary STAR data on K^- follow a different systematic than the rest of the points and also seem to deviate from the K_s^0 data. This could indicate a failure of proper particle identification in this momentum range.

Protons and antiprotons have been identified by PHENIX Collaboration up to 4.5 GeV/c and the final data were published very recently [62]. In contrast to the Goldstone bosons considered before, the mass of p and \bar{p} in our constituent quark picture is closer to the physical mass of 938 MeV and secondary protons and antiprotons are less abundant. Hence our calculation provides a satisfactory description of the spectra even between 1 and 2 GeV/c. This is true for all hadrons that are not Goldstone bosons. The crossover between the recombination and the fragmentation process is shifted upward for p and \bar{p} compared with pions, to around 6 GeV/c. We alert the reader to the apparent suppression of the fragmentation process below 6 GeV/c compared with re-

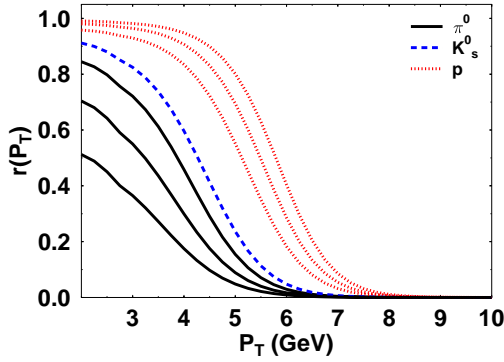


FIG. 5. (Color online) The ratio $r(P_T)=R/(R+F)$ of recombined hadrons to the sum of recombination and fragmentation for π^0 (solid line), K_s^0 (dashed line), and p (dotted lines). For protons and pions different impact parameters $b=0, 7.5$, and 12 fm (from top to bottom) are shown. K_s^0 is for $b=0$ fm only.

combination. This is much more prominent here than in the case of pions. In Fig. 5 we show the ratio $r(P_T)$ of recombined hadrons to the full calculation, defined in Eq. (91). The shift of the crossover to higher P_T from pions over kaons to protons is obvious. The 50% mark changes from 4 to 4.5 to 6 GeV/c.

Here we need to emphasize an important point regarding the perturbative calculation. The fragmentation functions are a nonperturbative input to these calculations, and are derived from other experiments. Most data about fragmentation functions are from e^+e^- annihilation experiments which do not allow to distinguish between quark and antiquark fragmentation. Quarks have to be created in pairs, so that only fragmentation functions like $D_{u+\pi \rightarrow p+p}$ can be deduced. Additional input from semiexclusive reactions helps to separate the contributions, but fragmentation functions still require improvement for applications in hadron interactions. The KKP parametrization seems to work well for π^0 production at RHIC [59] but we anticipate more problems for other hadrons, in particular for protons and antiprotons. This suggests a considerably larger theoretical uncertainty for the results from fragmentation of all hadrons other than pions. For this reason, and due to the lack of appropriate fragmentation functions, we do not show the fragmentation contribution for Φ , Ξ , and Ω in our calculations.

Our results for $\Lambda+\bar{\Lambda}$ include an equally large contribution from Σ^0 and $\bar{\Sigma}^0$. The preliminary STAR data are taken from Ref. [61]. For the multistrange hadron spectra $\Xi^-+\Xi^+$, $\Omega+\bar{\Omega}$, and Φ —which are supposed to have a pure $s\bar{s}$ valence structure—we present only recombination spectra. The strange hadron yields determine our value of the strange quark fugacity $\gamma_s=0.8$. Preliminary STAR data is available on $\Xi^-+\Xi^+$ [61] and $\Omega+\bar{\Omega}$ (minimum bias) [63]. We also show a calculation for an impact parameter of 10 fm which agrees well with the minimum bias $\Omega+\bar{\Omega}$ data. No spectra for Φ mesons at RHIC have been published so far.

The charged hadron spectrum $(h^++h^-)/2$ is shown separately in Fig. 6: pions, protons, antiprotons, and kaons are taken into account. This spectrum, including its impact parameter dependence, will be discussed in detail in the section on centrality dependence.

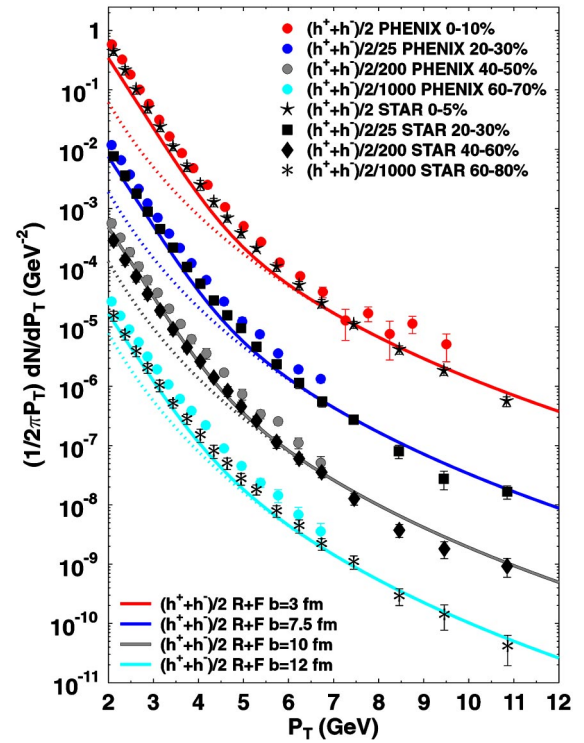


FIG. 6. (Color online) The spectrum of charged hadrons $(h^++h^-)/2$ for four different impact parameters 3, 7.5 (divided by 25), 10 (/200), and 12 fm(/1000) (from top to bottom) in comparison with data from STAR and PHENIX in different centrality bins. Contributions from fragmentation only (dotted) and the sum of recombination and fragmentation ($R+F$, solid lines) are shown.

In summary, our calculations using one fixed parameter set are consistent with all the currently existing data from RHIC and allow us to make predictions for future measurements.

B. Hadron ratios

In Fig. 7 we show hadron ratios. Only statistical errors are shown. The systematic errors can be quite large—we refer the reader to the cited experimental publications for further details.

One of the main motivations at the onset of our investigation was to find an explanation for the surprisingly large proton over pion ratios that are of the order of 1 above 1.5 GeV/c. The data on the p/π^0 and \bar{p}/π^0 ratios stem from PHENIX collaboration [62]. We have already shown in a previous publication [10] that recombination naturally provides a p/π^0 of order one for hadron transverse momenta up to 4 GeV. In addition, we predict that a sharp drop beyond 4 GeV/c should be seen when the fragmentation process takes over. The value predicted for the ratio in the fragmentation domain is about 0.1. At small transverse momenta, the statistical model describes the data well but continues to rise beyond 4 GeV/c.

The K^+/π^+ and K^-/π^- ratios have been measured by BRAHMS [64], and the K^-/K^+ ratio is compared to data from PHENIX [60]. For the statistical model we probe an additional strangeness fugacity and provide curves for values

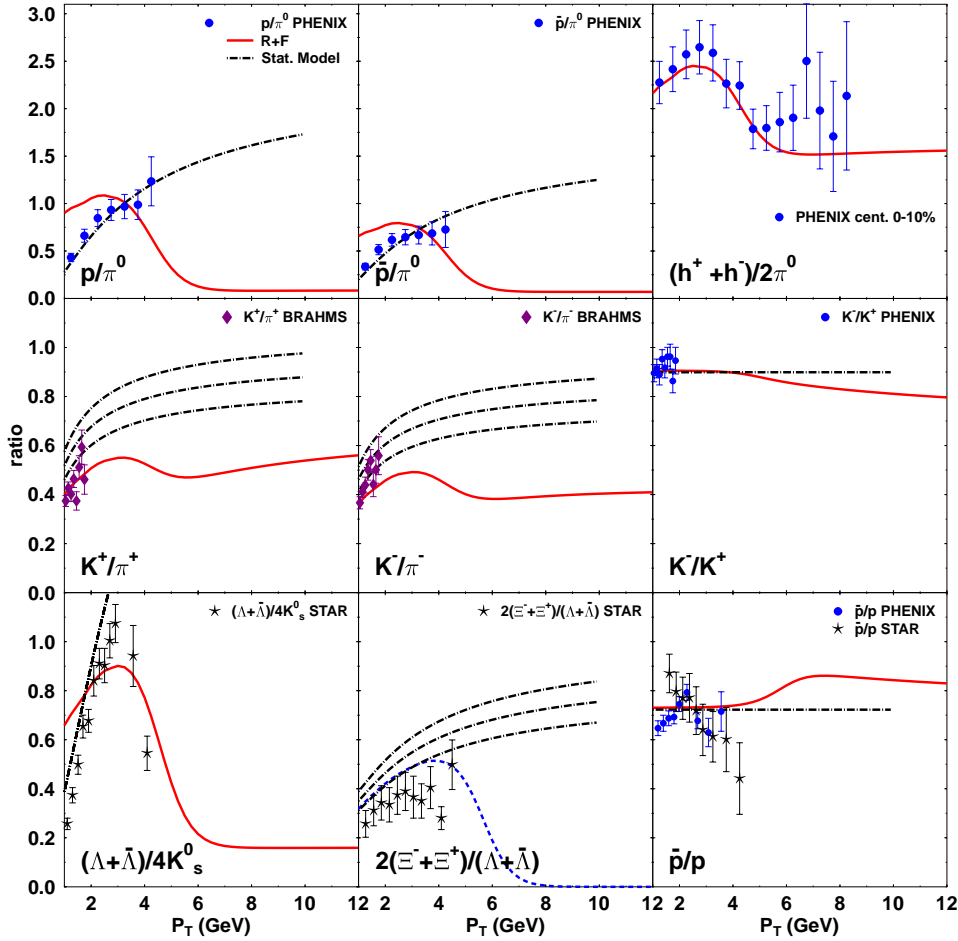


FIG. 7. (Color online) Hadron ratios p/π^0 , \bar{p}/π^0 , \bar{p}/p , K^+/π^+ , K^-/π^- , K^-/K^+ , $(\Lambda+\bar{\Lambda})/4K_s^0$, $2(\Xi^- + \Xi^+)/(\Lambda+\bar{\Lambda})$, and $2\pi^0/(h^+ + h^-)$ as functions of transverse momentum P_T . The calculation for Ξ baryons only takes into account recombination. We show data from STAR, PHENIX, and BRAHMS and results from the statistical model (dash-dotted lines). Where several curves for the statistical model are shown these are for different strangeness fugacities 1.0, 0.9, and 0.8 (from top to bottom).

of 1.0, 0.9, and 0.8. For the recombination part $\gamma_s=0.8$ was used as discussed above. The interesting feature of the preliminary \bar{p}/p data from STAR [65] and PHENIX [60] is that PHENIX implies a flat \bar{p}/p ratio up to 4 GeV/c, while STAR sees a decrease from 2 GeV/c on. (This may be related to the apparent surplus of K^- measured by STAR in the same momentum range, indicating a possible failure of charged particle identification beyond 2 GeV/c.) Our calculation predicts a flat ratio in this transverse momentum range in agreement with the PHENIX data. A linear sum of statistical and systematic errors is shown for the STAR data.

Preliminary results for the ratios $(\Lambda+\bar{\Lambda})/4K_s^0$ and $2(\Xi^- + \Xi^+)/(\Lambda+\bar{\Lambda})$ were also presented from STAR Collaboration [61]. Our calculations (for Ξ recombination only) are in rather good agreement. Recombination predicts a large peak in the Λ /kaon ratio and a sharp decrease beyond 4 GeV/c similar to the p/π^0 ratio. First indications of such a sharp transition can be seen in the STAR data. This observation supports the recombination picture including a transition to the fragmentation regime beyond 4 GeV/c.

For completeness we also show the ratio of charged hadrons to neutral pions reported by PHENIX [62] in comparison with our results. Our calculation agrees very well with the PHENIX data in the recombination region but slightly underestimates the ratio in the fragmentation region.

In summary, our calculations are in good agreement with the available RHIC data. The predicted decrease in the

proton/pion ratio, if confirmed, and first observations of a similar drop in the Λ /kaon ratio will be strong arguments in favor of the recombination+fragmentation picture.

C. Centrality dependence

Figures 8 and 9 show the centrality dependence of the π^0 and K_s^0 spectra. Final results in various centrality bins for π^0 have been published by PHENIX [52]. The K_s^0 data are preliminary results from STAR [61]. The impact parameter dependence of the charged hadron spectrum $(h^+ + h^-)/2$ was already shown in Fig. 6 with data from STAR [66] and PHENIX [67].

The impact parameter dependence of the parameters in our calculation was fixed by a fit to the π^0 data but it is consistent with the kaon and charged hadron data. We notice that with increasing impact parameter the hadrons from fragmentation come ever closer to the data points below the crossover point. Thus fragmentation becomes more and more important in peripheral collisions in accordance with our expectations. For the most peripheral bin in π^0 , with an impact parameter of 13.9 fm we refrained from extracting a recombination contribution. In principle, the data can be explained by fragmentation alone down to 2 GeV/c. We give a recombination contribution for $b=13$ fm although its contribution might be disputable already in this centrality bin.

Figure 5 shows the ratio of $r(P_T)$ for three different impact parameters (0, 7.5, and 12 fm) for protons and pions. The

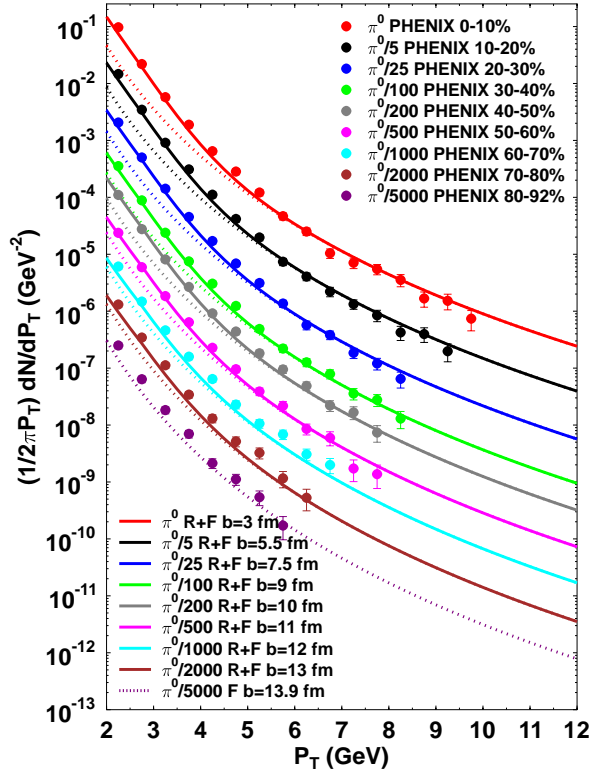


FIG. 8. (Color online) The spectrum of neutral pions for impact parameters 3, 5.5 (divided by 5), 7.5 (/25), 9 (/100), 10 (/200), 11 (/500), 12 (/1000), 13 (/2000), and 13.9 fm (/5000) (from top to bottom) in comparison with data from PHENIX in different centrality bins. Contributions from fragmentation only (dotted lines) and the sum of recombination and fragmentation (R+F, solid lines) are shown. 13.9 fm calculation is fragmentation (F) only.

systematics confirms that the crossover point shifts to smaller P_T for increasing b and that the weight of fragmentation becomes more and more important. In Fig. 10 we display the impact parameter dependence of the p/π^0 ratio. As expected, the proton/pion ratio is decreasing with increasing b in the recombination region and is unaltered where fragmentation is dominating.

It is an interesting question at which impact parameter the recombination mechanism becomes negligible for transverse momenta above 2 GeV/c. This will happen at smaller impact parameter for pions than for protons. Related to this issue is the question whether recombination contributes to hadron production at central rapidity in $p+A$ or $d+A$ reactions, where the produced matter is less dense. We still expect recombination to be an important mechanism at low P_T . However, there will probably be no chemical and thermal equilibration in the parton spectrum, and much less flow. The b dependence in Au+Au collisions is not a good basis for extrapolation since flow and equilibration seem to diminish only in very peripheral collisions. That makes it difficult to give quantitative predictions without data. However, we would expect that no recombination effects in pion production are visible above 2 GeV/c in $d+Au$ collisions.

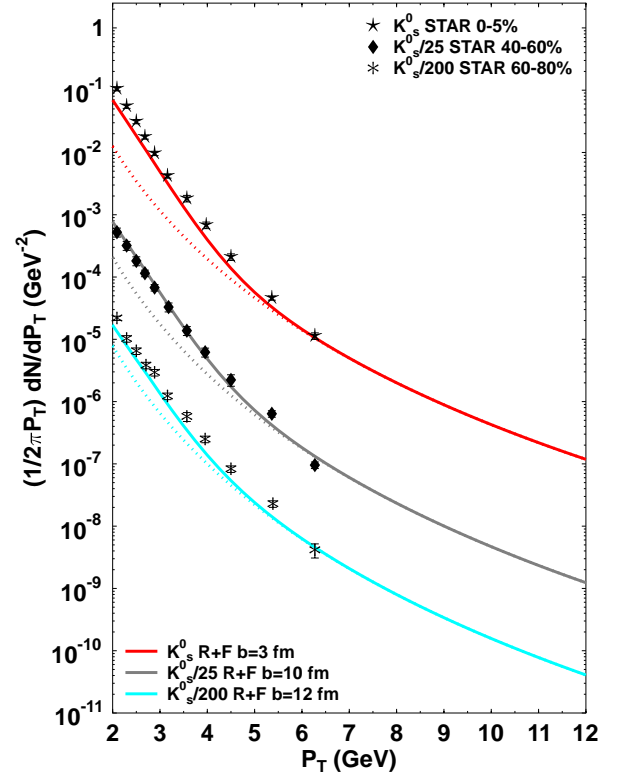


FIG. 9. (Color online) The spectrum of neutral kaons for impact parameters 3, 10 (/25), and 12 fm (/200) (from top to bottom) in comparison with data from STAR in different centrality bins. Contributions from fragmentation only (dotted lines) and the sum of recombination and fragmentation (R+F, solid lines) are shown.

D. Nuclear modification factors

The nuclear modification factor is defined as the ratio of the hadron yield in Au+Au collisions to the one in $p+p$ scaled with the number of collisions

$$R_{AA} = \frac{d^2N_{Au+Au}(b)/dP_T^2}{N_{coll}(b)d^2N_{p+p}/dP_T^2}. \quad (94)$$

Similarly one can consider scaled ratios of different centrality bins like central ($b_0=3$ fm) to peripheral

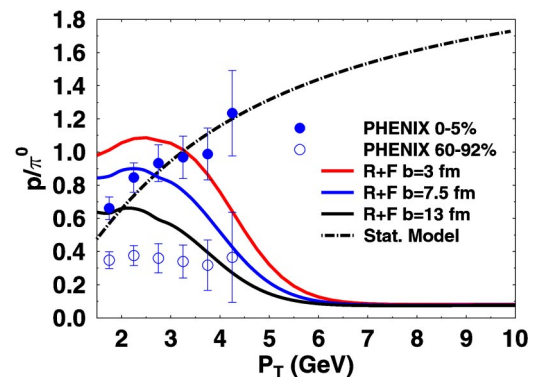


FIG. 10. (Color online) The ratio p/π^0 for three different impact parameters 3, 7.5, and 13 fm (solid lines, top to bottom) compared to the statistical model (dash-dotted line) and PHENIX data.

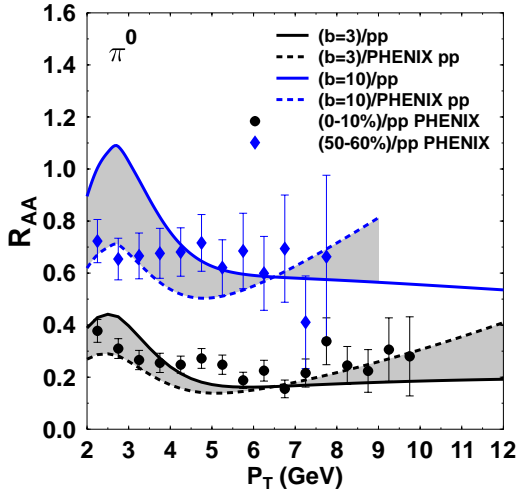


FIG. 11. (Color online) Nuclear modification factor R_{AA} for π^0 at impact parameters 3 (bottom) and 10 fm (top). Normalization by $p+p$ is via our own calculation (solid lines) or via PHENIX $p+p$ results (dashed lines). Data on R_{AA} are from PHENIX Collaboration with point-to-point errors only.

$$R_{CP} = \frac{N_{\text{coll}}(b)d^2N_{\text{Au+Au}}(b_0)/dP_T^2}{N_{\text{coll}}(b_0)d^2N_{\text{Au+Au}}(b)/dP_T^2}. \quad (95)$$

In Fig. 11 we show the nuclear modification factor for neutral pions for two impact parameters, $b=3$ and $b=10$ fm. We provide ratios taken both with our own $p+p$ calculation and with the $p+p$ results from PHENIX [59] and compare to final data from PHENIX [52]. We notice that there is an apparent uncertainty in the perturbative calculation which makes the two curves using our own $p+p$ calculation and the PHENIX $p+p$ results deviate. However, both curves are consistent with the data for central collisions. The problem is amplified for peripheral collisions, where the curve using our $p+p$ calculation overestimates R_{AA} below 4 GeV/c. The spread between both curves can be interpreted as a typical error to be expected in a lowest-order perturbative calculation. The nuclear modification factor for pions shows the strong jet quenching effect that suppresses the pion yield by about a factor of 5 for the highest P_T bins in central collision.

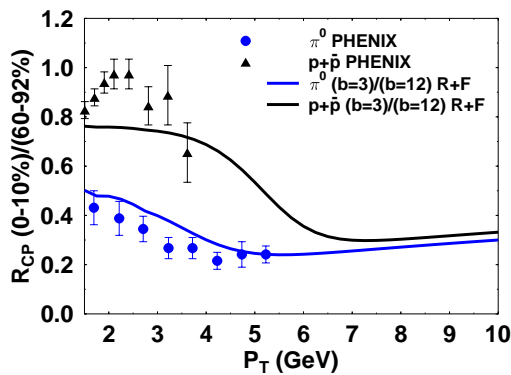


FIG. 12. (Color online) R_{CP} for neutral pions (bottom) and protons (top) given by the ratio of particle yields at impact parameters 3 and 12 fm compared to data from PHENIX.

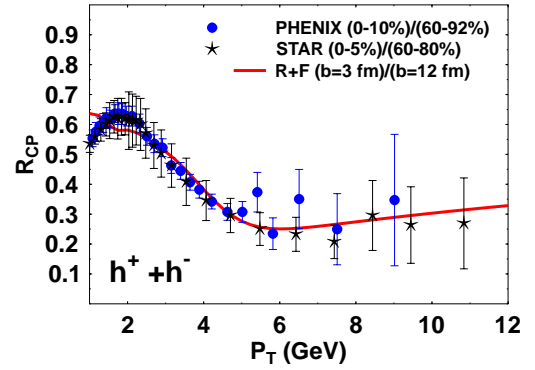


FIG. 13. (Color online) R_{CP} for charged hadrons given by the ratio of particle yields at impact parameters 3 and 12 fm compared to data from STAR and PHENIX.

Recombination predicts a slight increase below 4 GeV/c which can be observed in the data. However, recombination is not able to compensate the loss of pions through jet quenching at high P_T . In peripheral collisions jet quenching effects are much weaker.

Figure 12 displays the scaled ratio R_{CP} for neutral pions and protons. The ratio of impact parameters 3 and 12 fm is used and compared to data from PHENIX Collaboration [67]. The data for protons show R_{CP} to be between 0.8 and 1 below 4 GeV/c, which is quite surprising, considering the strong suppression suffered by the pions in that momentum domain. As already noticed above, recombination is more effective for protons than for pions. Therefore our calculation for the protons yields a similar value of 0.8 as observed by the experiment. This implies that protons from recombination make up for the loss suffered from jet quenching at intermediate transverse momenta. Our calculations predict sharp drops in R_{CP} and R_{AA} for protons and antiprotons beyond 4 GeV/c where fragmentation with jet quenching start to dominate.

In Fig. 13 we give R_{CP} for charged hadrons compared to data from STAR [68] and PHENIX [69]. The contribution from recombination below 4 GeV/c leads to a value of about 0.6 which is between the values for protons and pions. The

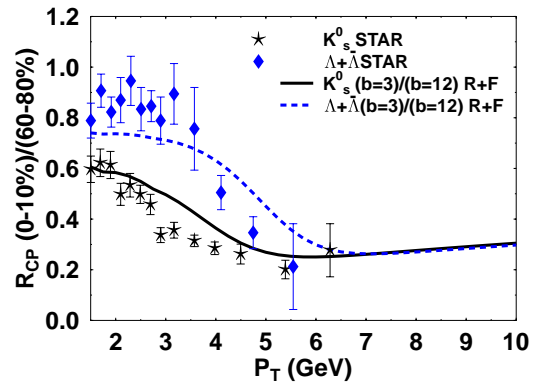


FIG. 14. (Color online) R_{CP} for K_s^0 (bottom) and $\Lambda+\bar{\Lambda}$ (top) given by the ratio of particle yields at impact parameters 3 and 12 fm compared to data from STAR.

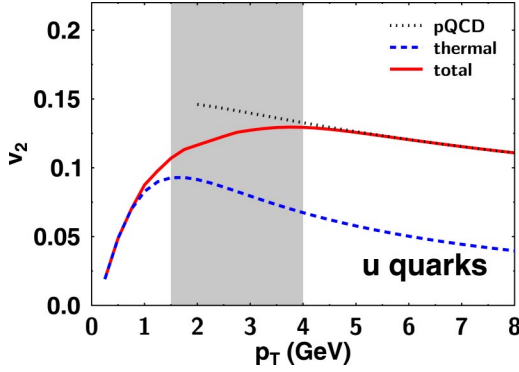


FIG. 15. (Color online) Elliptic flow v_2 in the parton phase as a function of transverse momentum p_T . The flow in the thermal phase (dashed line) and a pQCD calculation (dotted line) are shown. The solid line interpolates between the two domains. The shaded region shows the region where the interpolation takes place.

observed steep drop to the value attributed to jet quenching is well described by our theory.

Finally in Fig. 14 we compiled R_{CP} for K_s^0 and $\Lambda + \bar{\Lambda}$ together with data from STAR [61]. The different behaviors of mesons and baryons are again impressively confirmed. For the first time experimental data indicate that a steep decrease in R_{CP} for baryons will occur beyond 4 GeV/c. The data on $\Lambda + \bar{\Lambda}$ suggest a drop to the perturbative value even sharper than what our results show. This could be due to too few Λ baryons from fragmentation using this particular set of fragmentation functions [50].

E. Results on elliptic flow

Figure 15 shows the elliptic flow $v_2(p_T)$ of u quarks before hadronization. The contributions from jet quenching and from anisotropic flow in the thermal phase are shown separately as well. Due to the very different behavior in the two domains, v_2 is more sensitive to mechanisms which interpolate between the perturbative domain and the soft domain. The range of this theoretical uncertainty is highlighted by the shaded region in Fig. 15.

In Fig. 16 we provide results for π^+ . The contributions from fragmentation and recombination are shown separately. The full calculation interpolates between these two curves in the interval between 2 and 4 GeV/c. We also compare the result of a calculation using the δ -function approximation for the wave functions. As expected, the deviations are small. Our calculations agree with PHENIX data on v_2 of π^+ and π^- [57].

Our results on the particle dependence of elliptic flow are summarized in Fig. 17. One can see the different behavior of mesons and baryons by comparing protons with pions and kaons with Λ 's. v_2 for baryons saturates at a higher value than for mesons in the recombination domain. At higher P_T , when fragmentation takes over, the results rapidly approach each other. In our calculation, where we do not take into account the binding energies, we cannot resolve the splitting between protons and mesons coming from the mass difference. Nevertheless, the agreement with data from PHENIX [57] and preliminary data from STAR [70] is good. In Fig.

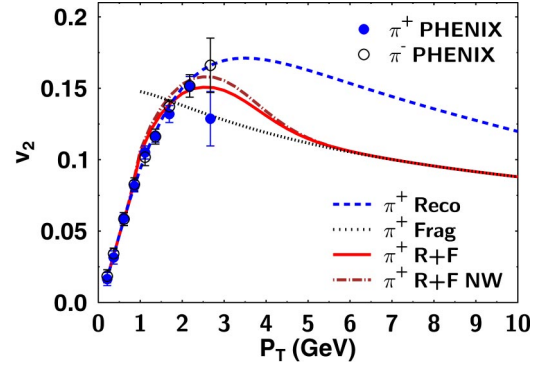


FIG. 16. (Color online) v_2 for positively charged pions. We show recombination only (dashed line), fragmentation only (dotted line), and the full calculation (solid line). The result of a calculation in the δ -function approximation (NW) for the wave function is also shown (dash-dotted line). Data are taken from PHENIX Collaboration [57].

18 v_2 for charged hadrons is compared with preliminary STAR data [71]. This is interesting since for charged hadrons the measurements extend up to 7 GeV/c and constrain v_2 in the pQCD domain. Note that in this case v_2 was extracted by STAR from four particle correlations. This is supposed to reduce nonflow effects to v_2 [72] in comparison with the usual reaction plane analysis.

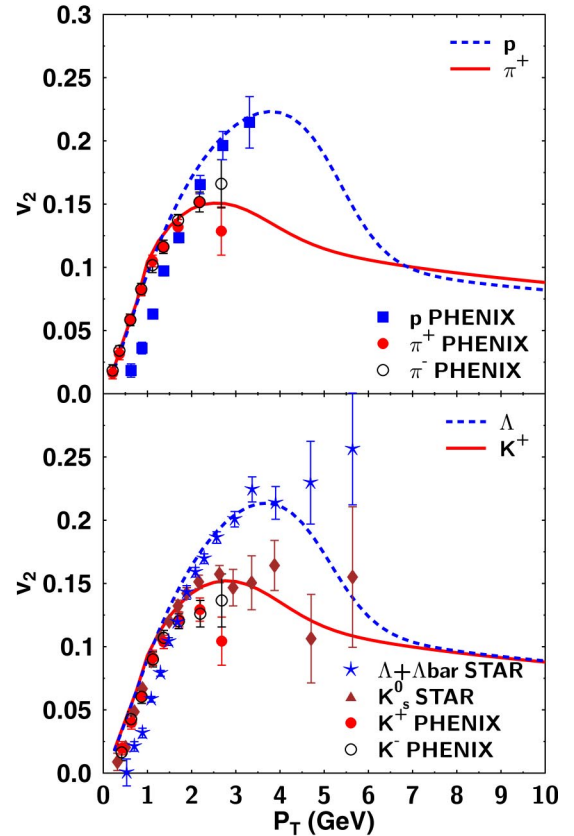


FIG. 17. (Color online) Upper panel: anisotropic flow for p and π^+ compared to PHENIX data [57]. Lower panel: v_2 for K^+ and $\Lambda + \bar{\Lambda}$ compared to preliminary STAR data ($\Lambda + \bar{\Lambda}, K_s^0$) [70] and PHENIX data (K^+, K^-) [57].

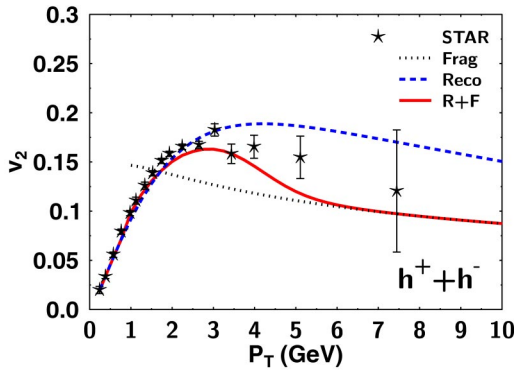


FIG. 18. (Color online) v_2 for charged hadrons. Again we show the contributions from different mechanisms as in Fig. 16. Data are preliminary and taken from STAR Collaboration.

In Fig. 19 we test the scaling law from Eq. (89) for protons and pions. Protons and pions follow one universal curve below 1.5 GeV/c, which is very similar to the flow of thermal partons given in Fig. 15. Beyond 1.5 GeV/c we predict a transition to the values given by pQCD. The scaling law is no longer valid in that domain.

We would like to emphasize that we expect modifications from other hadronization mechanisms in the region where we interpolate between the recombination and the fragmentation dominated domains. These could be quite important in the case of v_2 and alter the results in the interpolation region, e.g., they could smoothen the transition between both domains. Interactions in the hadronic phase could alter v_2 further.

VI. CONCLUSIONS

In this work we have presented extensive evidence that recombination is the dominant hadronization mechanism for central Au+Au collisions at RHIC up to about 4 GeV/c for pions and 6 GeV/c for protons. We have described a covariant framework that permits the calculation of recombination from a dense thermal parton phase using light-cone wave

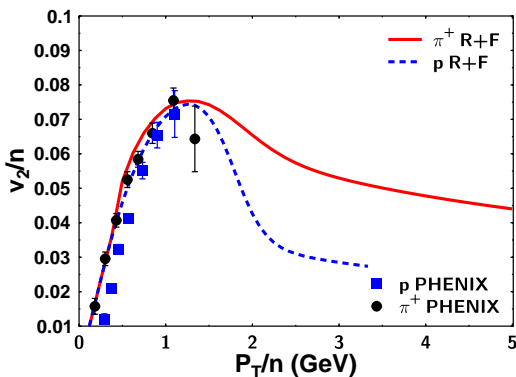


FIG. 19. (Color online) The anisotropy v_2/n for pions (bottom) and protons (top) as a function of transverse momentum p_T/n using the scaling law (89) with $n=2$ for pions and $n=3$ for protons. Data points are pions and protons from PHENIX using the same scaling law.

functions for the produced hadrons. This formalism is adequate for momenta much larger than the non-perturbative scales involved. At lower energies, energy and entropy conservation pose a serious problem, the solution of which requires a dynamical, rather than purely kinematic, treatment of the recombination process. We have found that, for practical purposes, hadron spectra are well described down to transverse momenta of 2 GeV/c for Goldstone bosons (π, K) and 1 GeV/c for other hadrons.

Recombination competes with fragmentation from perturbatively scattered partons. The large energy loss of these partons leads to sizable quenching factors, which reduce the fragmentation contribution and cause it to be buried under soft physics at scales which one would not generally attribute to soft physics. However, 4 GeV/c in the pion and 6 GeV/c in the proton spectrum correspond to a transverse momentum of only 2 GeV/c on an average for the coalescing partons.

The interplay of recombination and fragmentation leads to interesting effects in particle ratios and nuclear modification factors. The proton/pion ratio is naturally around 1 in the recombination regime. For protons the unquenching effect by recombination below 4 GeV/c is so strong that essentially no nuclear suppression can be observed at all in this momentum range. For the proton/pion ratio and suppression factors R_{AA} and R_{CP} we expect a sharp drop beyond 4 GeV/c indicating the beginning of the perturbative regime.

For the azimuthal asymmetry v_2 , our calculations describe the data well. The different behavior of baryons and mesons above 1 GeV/c can be explained. The scaling law (89), derived from the recombination formalism, is consistent with data up to 1.5 GeV/c. We predict a violation of this scaling law at higher values, coming from perturbative QCD.

In this publication we have only considered single hadron production and neglected correlations in the hadron emission pattern. The yield of secondary hadrons, when triggering on a leading hadron, is a promising quantity to provide more information about the underlying hadronization mechanism.

With fragmentation and energy loss alone, no consistent explanation involving all hadron species can be given. In contrast, we are able to describe most available RHIC data on spectra, ratios, nuclear suppression, and elliptic flow of hadrons, including their impact parameter dependence, for transverse momenta above 1–2 GeV/c—for v_2 even down to very low P_T —consistently with a very small number of globally adjusted parameters. As input for the recombination process we use a dense phase of partons with temperature $T=175$ MeV and radial flow velocity $v_T=0.55c$ at hadronization time 5 fm. All RHIC data shown in this work are consistent with the existence of such a phase.

ACKNOWLEDGMENTS

This work was supported by RIKEN, Brookhaven National Laboratory, DOE Grant Nos. DE-FG02-96ER40945 and DE-AC02-98CH10886, and by the Alexander von Humboldt Foundation. We thank M. Stratmann for providing a code for Λ fragmentation. We are grateful to D. d'Enterria, S. D. Ellis, D. Hardtke, U. Heinz, P. Jacobs, Z. W. Lin, D. Molnar, J. Velkovska, and X. N. Wang for useful discussions.

- [1] K. Adcox *et al.*, PHENIX Collaboration, Phys. Rev. Lett. **88**, 022301 (2002); C. Adler *et al.*, STAR Collaboration, *ibid.* **90**, 082302 (2003).
- [2] J. D. Bjorken, FERMILAB-PUB-82-059-THY (1982); M. H. Thoma and M. Gyulassy, Nucl. Phys. **B351**, 491 (1991); X. N. Wang and M. Gyulassy, Phys. Rev. Lett. **68**, 1480 (1992); M. Gyulassy and X. Wang, Nucl. Phys. **B420**, 583 (1994); R. Baier, Y. L. Dokshitzer, A. H. Mueller, S. Peigne, and D. Schiff, *ibid.* **B483**, 291 (1997); B. G. Zakharov, JETP Lett. **65**, 615 (1997); M. Gyulassy, P. Levai, and I. Vitev, Phys. Rev. Lett. **85**, 5535 (2000); U. A. Wiedemann, Nucl. Phys. **B588**, 303 (2000).
- [3] R. Baier, Y. L. Dokshitzer, A. H. Mueller, and D. Schiff, J. High Energy Phys. **0109**, 033 (2001).
- [4] B. Müller, Phys. Rev. C **67**, 061901 (2003).
- [5] K. Adcox *et al.*, PHENIX Collaboration, Phys. Rev. Lett. **88**, 242301 (2002).
- [6] C. Adler *et al.*, STAR Collaboration, Phys. Rev. Lett. **86**, 4778 (2001).
- [7] C. Adler *et al.*, STAR Collaboration, Phys. Rev. Lett. **89**, 092301 (2002).
- [8] K. Adcox *et al.*, PHENIX Collaboration, Phys. Rev. Lett. **89**, 092302 (2002).
- [9] I. Vitev and M. Gyulassy, Phys. Rev. C **65**, 041902 (2002).
- [10] R. J. Fries, B. Müller, C. Nonaka, and S. A. Bass, Phys. Rev. Lett. **90**, 202303 (2003).
- [11] V. Greco, C. M. Ko, and P. Levai, Phys. Rev. Lett. **90**, 202302 (2003).
- [12] Z. W. Lin and C. M. Ko, Phys. Rev. Lett. **89**, 202302 (2002).
- [13] S. A. Voloshin, Nucl. Phys. **A715**, 379c (2003).
- [14] D. Molnár and S. A. Voloshin, Phys. Rev. Lett. **91**, 092301 (2003).
- [15] Z. Lin and D. Molnár, nucl-th/0304045.
- [16] P. Sorensen, STAR Collaboration, J. Phys. G (to be published), nucl-ex/0305008.
- [17] J. F. Owens, Rev. Mod. Phys. **59**, 465 (1987).
- [18] J. C. Collins and D. E. Soper, Nucl. Phys. **B194**, 445 (1982).
- [19] B. A. Kniehl, G. Kramer, and B. Pötter, Nucl. Phys. **B582**, 514 (2000).
- [20] X. F. Guo and X. N. Wang, Phys. Rev. Lett. **85**, 3591 (2000); Nucl. Phys. **A696**, 788 (2001).
- [21] E. Wang and X. N. Wang, Phys. Rev. Lett. **89**, 162301 (2002).
- [22] X. N. Wang, nucl-th/0305010.
- [23] K. P. Das and R. C. Hwa, Phys. Lett. **68B**, 459 (1977); **73**, 504(E) (1978); R. G. Roberts, R. C. Hwa, and S. Matsuda, J. Phys. G **5**, 1043 (1979).
- [24] E. M. Aitala *et al.*, E791 Collaboration, Phys. Lett. B **371**, 157 (1996).
- [25] J. C. Anjos, J. Magnin, and G. Herrera, Phys. Lett. B **523**, 29 (2001).
- [26] E. Braaten, Y. Jia, and T. Mehen, Phys. Rev. Lett. **89**, 122002 (2002).
- [27] C. Gupta, R. K. Shivpuri, N. S. Verma, and A. P. Sharma, Nuovo Cimento A **75**, 408 (1983).
- [28] T. Ochiai, Prog. Theor. Phys. **75**, 1184 (1986).
- [29] T. S. Biro, P. Levai, and J. Zimanyi, Phys. Lett. B **347**, 6 (1995); J. Phys. G **28**, 1561 (2002).
- [30] R. C. Hwa and C. B. Yang, Phys. Rev. C **66**, 025205 (2002).
- [31] V. Greco, C. M. Ko, and P. Levai, Phys. Rev. C **68**, 034904 (2003).
- [32] R. Rapp and E. V. Shuryak, Phys. Rev. D **67**, 074036 (2003).
- [33] O. Kaczmarek, F. Karsch, E. Laermann, and M. Lutgemeier, Phys. Rev. D **62**, 034021 (2000); A. Peshier, B. Kämpfer, and G. Soff, *ibid.* **66**, 094003 (2002).
- [34] J. Casalderrey Solana and E. V. Shuryak, hep-ph/0305160.
- [35] R. Scheibl and U. W. Heinz, Phys. Rev. C **59**, 1585 (1999).
- [36] U. A. Wiedemann, B. Tomasik, and U. W. Heinz, Nucl. Phys. **A638**, 475C (1998).
- [37] C. Adler *et al.*, STAR Collaboration, Phys. Rev. Lett. **87**, 082301 (2001); K. Adcox *et al.*, PHENIX Collaboration, *ibid.* **88**, 192302 (2002).
- [38] C. B. Dover, U. W. Heinz, E. Schnedermann, and J. Zimanyi, Phys. Rev. C **44**, 1636 (1991).
- [39] F. Cooper and G. Frye, Phys. Rev. D **10**, 186 (1974).
- [40] V. L. Chernyak and A. R. Zhitnitsky, JETP Lett. **25**, 510 (1977); G. P. Lepage and S. J. Brodsky, Phys. Lett. B **87**, 359 (1979); Phys. Rev. Lett. **43**, 545 (1979); **43**, 1625(E) (1979); A. V. Efremov and A. V. Radyushkin, Theor. Math. Phys. **42**, 97 (1980); Phys. Lett. B **94**, 245 (1980); V. L. Chernyak and A. R. Zhitnitsky, Phys. Rep. **112**, 173 (1984).
- [41] F. Karsch, Nucl. Phys. **A698**, 199 (2002).
- [42] W. Broniowski and W. Florkowski, Phys. Rev. Lett. **87**, 272302 (2001); W. Broniowski, A. Baran, and W. Florkowski, Acta Phys. Pol. B **33**, 4235 (2002).
- [43] P. Braun-Munzinger, D. Magestro, K. Redlich, and J. Stachel, Phys. Lett. B **B518**, 41 (2001).
- [44] N. Xu and M. Kaneta, Nucl. Phys. **A698**, 306 (2002).
- [45] R. J. Fries, B. Müller, and D. K. Srivastava, Phys. Rev. Lett. **90**, 132301 (2003).
- [46] D. K. Srivastava, C. Gale, and R. J. Fries, Phys. Rev. C **67**, 034903 (2003).
- [47] K. J. Eskola and K. Tuominen, Phys. Rev. D **63**, 114006 (2001); G. G. Barnafoldi, G. Fai, P. Levai, G. Papp, and Y. Zhang, J. Phys. G **27**, 1767 (2001).
- [48] M. Luo, J. Qiu, and G. Sterman, Phys. Lett. B **279**, 377 (1992); J. Qiu and G. Sterman, Int. J. Mod. Phys. E **12**, 149 (2003).
- [49] E. V. Shuryak, Phys. Rev. C **66**, 027902 (2002).
- [50] D. de Florian, M. Stratmann, and W. Vogelsang, Phys. Rev. D **57**, 5811 (1998).
- [51] S. A. Bass, B. Müller, and D. K. Srivastava, Phys. Lett. B **551**, 277 (2003).
- [52] S. S. Adler, PHENIX Collaboration, Phys. Rev. Lett. **91**, 072301 (2003); K. Reygers, PHENIX Collaboration, http://www.phenix.bnl.gov/phenix/WWW/publish/enterrria/AuAu_pi0_200GeV_data/
- [53] X. N. Wang, Phys. Rev. C **63**, 054902 (2001).
- [54] M. Gyulassy, I. Vitev, and X. N. Wang, Phys. Rev. Lett. **86**, 2537 (2001).
- [55] E. Schnedermann, J. Sollfrank, and U. Heinz, Phys. Rev. C **48**, 2462 (1993).
- [56] P. Huovinen, P. F. Kolb, U. Heinz, P. V. Ruuskanen, and S. Voloshin, Phys. Lett. B **503**, 58 (2001).
- [57] S. S. Adler *et al.*, PHENIX Collaboration, nucl-ex/0305013.
- [58] D. Zschesche, S. Schramm, J. Schaffner-Bielich, H. Stöcker, and W. Greiner, Phys. Lett. B **547**, 7 (2002).

- [59] S. S. Adler *et al.*, PHENIX Collaboration, hep-ex/0304038.
- [60] T. Chujo, PHENIX Collaboration, Nucl. Phys. **A715**, 151c (2003).
- [61] H. Long, STAR Collaboration, J. Phys. G (to be published).
- [62] S. S. Adler *et al.*, PHENIX Collaboration, nucl-ex/0305036.
- [63] C. Suire, STAR Collaboration, Nucl. Phys. **A715**, 470c (2003).
- [64] J. H. Lee, BRAHMS Collaboration, Talk at SQM 2003, J. Phys. G (to be published).
- [65] G. J. Kunde, STAR Collaboration, Nucl. Phys. **A715**, 189c (2003).
- [66] J. Adams *et al.*, STAR Collaboration, nucl-ex/0305015.
- [67] J. Velkovska, PHENIX Collaboration, Talk at SQM 2003, J. Phys. G (to be published).
- [68] J. L. Klay, STAR Collaboration, Nucl. Phys. **A715**, 733c (2003).
- [69] S. Mioduszewski, PHENIX Collaboration, Nucl. Phys. **A715**, 199c (2003).
- [70] R. Snellings, STAR Collaboration, J. Phys. G (to be published), nucl-ex/0305001.
- [71] A. Tang, STAR Collaboration, Talk at CIPANP 2003, <http://www.phenix.bnl.gov/WWW/publish/nagle/CIPANP/>
- [72] N. Borghini, P. M. Dinh, and J. Y. Ollitrault, Phys. Rev. C **64**, 054901 (2001).